Synthesis, characterization and biomedical applications of PHB, PHBV coated silver nanoparticles (Ag NPs)

A DISSERTATION REPORT SUBMITTED IN PARTIAL FULFILMENT OF THE REQUIREMENTS FOR THE DEGREE OF

Master of Technology

(Nanotechnology)

By

Krishan Kumar

17551005

UNDER THE SUPERVISION OF

Dr. Krishna Mohan Poluri

&

Dr. Saugata Hazra

Centre of Nanotechnology

IIT Roorkee

Roorkee-247667 (India)

2019

CANDIDATE'S DECLARATION

I hereby solemnly declare that the work presented in dissertation report entitled "**Synthesis, characterization and biomedical applications of renewable Bio-plastics (3-PHB, PHBV) encapsulated/ coated silver nanoparticles"** submitted in partial fulfillment of the requirements for the award of the degree of **Master of Technology in Nanotechnology, Indian Institute of Technology Roorkee** is an authentic record of my work carried out under the supervision of **Dr. Krishna Mohan Poluri** & **Dr. Saugata Hazra**, Centre of Nanotechnology, IIT Roorkee. The matter embodied in this thesis has not been submitted by me for the award of any other degree.

Krishan Kumar

Enroll. 17551005

Date: 27.05.2019

CERTIFICATE

This is to certify that the above statement made by the student is correct to the best of my knowledge.

Dr. Krishna Mohan Poluri

Supervisor

Associate Professor
Centre of Nanotechnology,
Indian Institute of Technology,
Roorkee-247667, INDIA.

Dr. Saugata Hazra

Supervisor

Assistant Professor
Centre of Nanotechnology,
Indian Institute of Technology,
Roorkee-247667, INDIA.

Abstract

Bioplastics-capped silver nanoparticles may be anti-bacterial agents, or a general antimicrobial agent at broad spectrum as we are finding more and more applications of green, renewable, cost-effective biopolymers from microorganisms. Highly pathogenic, biofilm producing bacterial strains, e.g. *S.aureus* their drug-resistance nature, and support from the extracellular matrix may result in a complex illness that is very tough to cure. Metallic nanoparticles e.g. encapsulated silver (Ag) NPs have already proven to be effective against these bacteria. However, their biocompatibility and stability are some of the major disputes which should be addressed for their efficient utilization in the biomedical field. PHB biopolymer is green (renewable), degraded within the body (biodegradable) to non-toxic (biocompatible) by-products and has known applications in the field of biomedicine.

Chapter 1 is the basic introduction of the field, past discoveries to biomedical future of poly-hydroxybutyrates e.g. 3-PHB and PHBV biopolymers. It is also pointing towards the objectives of the study. Natural polymers alone are not very thermostable but their nanocomposites may have better mechanical and thermal properties.

Chapter 2 is the literature review and summarizing the what is already known about PHB and PHBV and what is nanotechnology, how nanomaterial differ from bulk in terms of their properties and applications. Also, this chapter contains references to all known green methods that have been used by people from time to time to synthesize nanoparticles of PHA alone or with metals.

Chapter 3 summarizes the techniques and instruments that are being utilized during the study. It includes UV-Vis/ FTIR spectroscopy, DLS/zeta sizer, SEM, TEM, XRD, TGA and SPM analysis for characterizations of 3-PHB, PHBV encapsulated nanoparticles.

Chapter 4 contain results of the characterization of nanoparticles, all experiments needed to study the effects of these freshly prepared nanoparticles of encapsulated silver over bacterial cells e.g. *P.aeruginosa, S.aureus,* and *B.thuringiensis* mainly and A549 alveolar adenocarcinoma cells of humans.

Chapter 5 contain Concluding Remarks and Future Perspectives for further study to explore their activity against e.g. fungi or viruses.

This study is about the instant chemical reduction of $AgNO_3$ and synthesis of PHB or PHBV (green renewable biopolymer) encapsulated silver nanoparticles e.g. PHB and PHBV stably encapsulate Ag atoms from $AgNO_3$ by using $NaBH_4$ as a reducing agent. The method described is found to be effective, simple, and instant. Synthesized nanoparticles are very small in size (2-25 nm) with very good stability in original colloidal solution form (zeta potential ~ 40 mV). These nanoparticles have been found to be efficiently removing *S.aureus, B.thuringiensis,* and *P.aeruginosa, E.coli,* and *S.epidermidis*like bacterial species and further intervention may possibly lead to the revelation of their potential as antibacterial therapeutics against biofilms. PHBV-Ag NPs are found to be more effective due to their smaller size than PHB-Ag NPs, and, having better nano-characteristics e.g. more surface roughness.

Owing to GRAS status, they can be used to enhance the antibiotic abilities of the silver nanoparticles. Hence, this study legitimately provides assurance that the PHB encapsulated silver NPs holds a great promise in this novel antimicrobial field for biomedical applications, e.g. antimicrobial, anti-fouling coatings of food packets and dressing applied to the wounds to suppress infections at sites of open injury. Other Possible Applications may be in **medicine**, in **pharmacology** and in the **packaging** of food, sprayed foils for fast foods, and fibers.

Chapter 1

Introduction

Highly pathogenic, biofilm producing bacterial strains, their drug-resistance nature, and support from the extracellular matrix may result in a complex contagious malady that is very tough to cure [1]. Metallic nanoparticles (NP) e.g. encapsulated silver (Ag) NPs have proven to be effective against these bacteria [2]. These biopolymers are green (renewable), degraded within the body (biodegradable) to non-toxic (biocompatible) by-products [3].

Polyhydroxyalkanoates (PHA) are food storage linear polyesters, biocompatible and biodegradable due to their origin from bacteria, which could utilize waste under unbalanced growth conditions. They are found to be good carriers for drug delivery and possess unique physiochemical, thermoplastic, and mechanical properties **(Fig. 1.1)** [3, 4]. Originally, natural materials had restricted shelf lives; therefore, plastics came into the picture and were developed to replace them. Today, plastics are used almost everywhere for biomedical as well as synthetic applications e.g. packaging and raw material. However, because of the non-biodegradable nature of most of the plastics, their use poses a serious threat to the environment [5]. Poly-hydroxybutyrate (PHB) is a biopolymer present in all living organisms. Commercial company 'Biomer' produces PHB pellets and can be used by bacteria and fungi as a food source. PHA polymers degradation occurs by surface erosion [6]. PHAs are found to be applicable in nanomedicine the field as biodegradable drug carriers, anti-cancer targeted therapy and biocompatible implants for tissue engineering scaffolds [3-7].

PHA's tissue scaffolding materials

Suture TephaFLEX® was first ever approved product of PHB by FDA [4], pulmonary artery and valves made from combined the polymer of polyglycolic acid (PGA) and PHB [8]. 3-PHB and PHBV (PHAs) are hydrophobic, piezoelectric biopolymers, thermo-processable, biocompatible, crystalline, and linear polyesters in nature, therefore, PHA particles may be utilized as drug carriers as microcapsules and NPs [9]. In the last decade, nanotechnology has emerged as an extremely novel and powerful approach to combat the issue of multi-drug resistance as nanomedicine. Various nanomaterials being utilized in healthcare and biomedical applications [6-10].

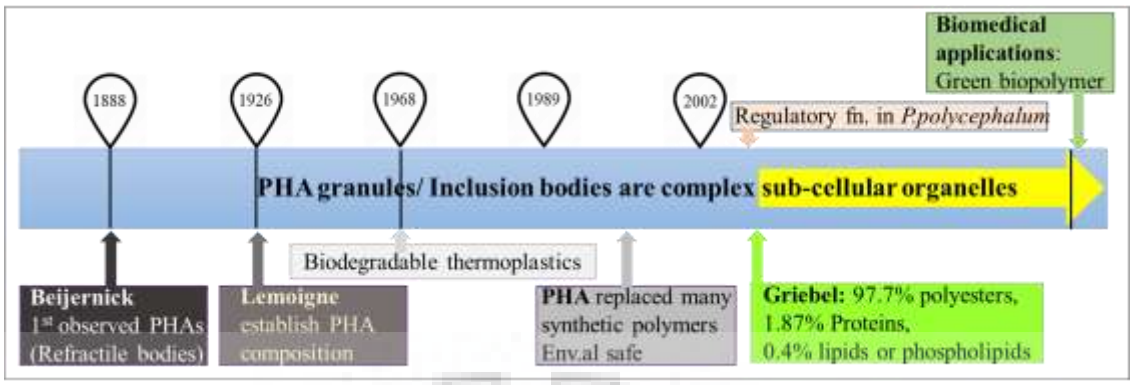

Figure 1.1: PHA (bio-plastic) major discoveries and route map to biomedical applications.

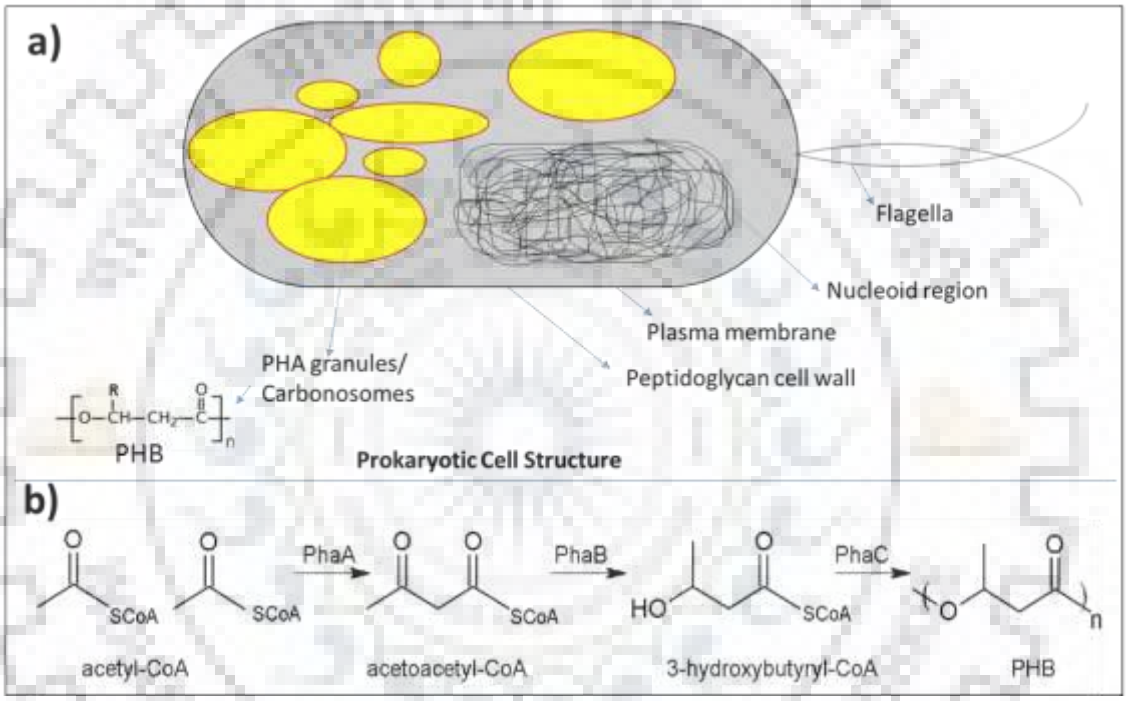

Figure 1.2: Biosynthesis of the green polymer by PhaC (condensation reaction) from acetoacetyl-CoA and storage inside bacterial "carbonosomes" granules [7].

Their unique physiochemical properties have enabled their use in various types of nanocomposites formulations [8-10]. Although there are many biological and physical techniques to synthesize polymer capped silver nanoparticles, but, the chemical reduction synthesis of silver nanoparticles is instant and appears to be the most promising technique owing to its facile methodology, easy reproducibility, and intact antibacterial properties of nanoparticles **(Table 2.2)** [11]. In the present study, encapsulated Ag NP (renewable biopolymer PHB or PHBV encapsulated silver NPs) were successfully formed using a reduction approach without employing any other toxic surfactants [12].

Till date, the Ag-NPs are most fascinating since they are least toxic to humans, easily reproducible, and antimicrobial agents against fungi, algae, and bacteria [13]. However, Ag-NPs may undergo aggregation after reduction of metal salt, thus can be misplaced in their physiochemical characteristics [14]. Therefore, we require a green encapsulating agent and PHAs like PHB, PHBV came into the picture to improve shelf-life of silver nanoparticles. Also, PHB is normally present in our blood so, the chances of immune recognition are minimized, thus, having a large number of biomedical applications [5, 7-10]. Generally, the synthesis mechanism of nanometre-sized metal nanoparticles includes: (i). the activation phase in which metal ion reduced and nucleation happens, (ii). the development and growth via either oriented aggregation or Ostwald's ripening including spontaneous mingle of the dwarf adjacent NPs forming a big particle, and (iii). the termination providing the final shape of the NPs [15].

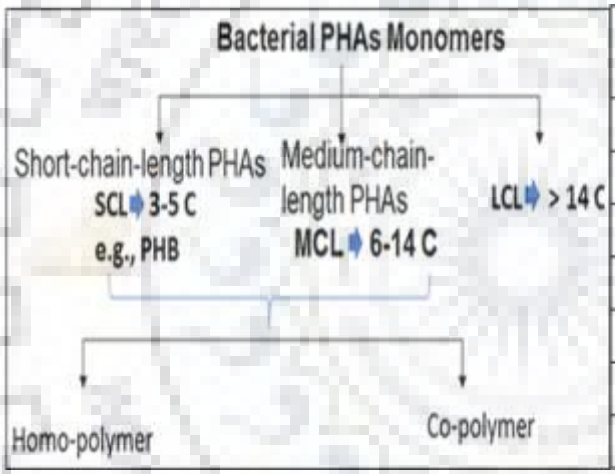

C-atoms	R-group	PHA
4	Methyl	Poly-3-hydroxybutyrate
5	Ethyl	Poly-3-hydroxyvalerate
6	Propyl	Poly-3-hydroxyhexanoate
7	Butyl	Poly-3-hydroxyheptanoate
8	Pentyl	Poly-3-hydroxyoctanoate
9	Hexyl	Poly-3-hydroxynonanoate
10	Heptyl	Poly-3-hydroxydeconate

Figure 1.3: Classification of PHAs based on C-chain length and composition.

Polymeric stabilized nanoparticles as wound dressings provide impeccable moisture environment for healing as well as protects the wound from further deterioration. These nanocomposites, when combined with novel antimicrobial agents, such as capped-silver nanoparticles, may impart a synergistic effect in the wound healing applications [16], also may be utilized in-vivo since there are no toxic degradation products of biopolymers (biocompatible and biodegradable). Silver nanoparticles embedded in a polymer hydro-NPs opens up new avenues for wound healing in the biomedical sector. Thus, a combination of PHB or PHBV and silver nanoparticles vow a great undertaking towards the development of a novel wound care dressings with antibacterial effect against chronic wounds [6, 17].

Polyhydroxyalkonates are having novel applicability in the nanomedicine field as biodegradable drug carriers, coating over medical implants, anti-cancer targeted therapy agents for drugs, and biocompatible implants of tissue scaffolds [9, 12].

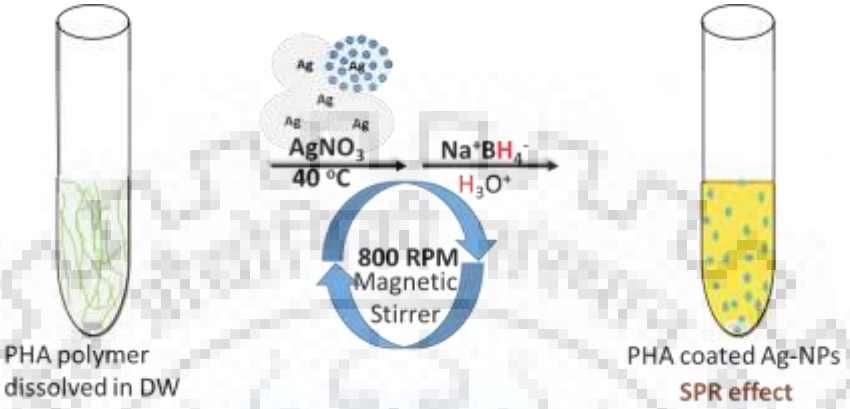

Figure 1.4: "Brust" method of NP synthesis: Green polymer encapsulated silver nanoparticles showing modified optical properties of bulk materials in nanoparticle form.

1.1 Scope of thesis

In the study, PHB or PHBV capped/ encapsulated silver nanoparticles were synthesized using instant chemical reduction ("brust" method). These nanoparticles were investigated and evaluated for their applicability in bacterial culture growth inhibition and their broad-spectrum antimicrobial activity over both gram-positive and gram-negative bacteria. Also, the changes in morphology of bacterial cells were seen under FE-SEM after fixing the bacterial cells in 2.5% glutaraldehyde solution. Hence, this study provides an insight into the role of nanobiotechnology in developing novel antimicrobial agents for wound healing applications. However, silver nanoparticles tend to aggregate in the absence of a befitting and stabilizing capping agent. Therefore, biocompatible polymers (PHAs e.g. PHB, PHBV) with attractive physiological and biological properties are being employed to cap nanoparticles that have applicability in biomedical applications. Also, the degradation kinetics of these green biopolymers (PHA) in vivo resulted in natural non-toxic monomers, suggesting they can show novel controlled drug releasing utility, targeted carriers, medical device materials which need not be removed after treatment, and thus, they may have major advances in applications of tissue engineering, healing, and growth.

1.2 Specific objectives

- To encapsulate PHB or PHBV over silver nanoparticles (PHB- or PHBV- coated Ag NPs) using green approach (UV or Microwave), instant chemical synthesis method and their nano-characterization (UV-Vis, DLS, Zeta potential, SEM, TEM, FTIR, XRD, TGA).
- Evaluation and comparison of antimicrobial properties of biopolymer (PHB, PHBV) encapsulated Ag NPs against the biofilm producing bacteria and human alveolar adenocarcinoma cells (A549) using MTS assay.

Chapter 2

Review of literature

2.1 Nanotechnology: Overview

Nanotechnology has gained momentum in recent years due to its vast applicability and potential in biomedical field. The prefix "nano" for materials having size range (1-100 nm in single dimension) are considered as nanomaterial [15]. They are having modified chemical and physical characteristics **(Fig. 2.1)**. Their enhanced capability to cross the blood-brain barrier is some of the attractive properties which are useful in the biomedical and other applications (**Table 2.1**).

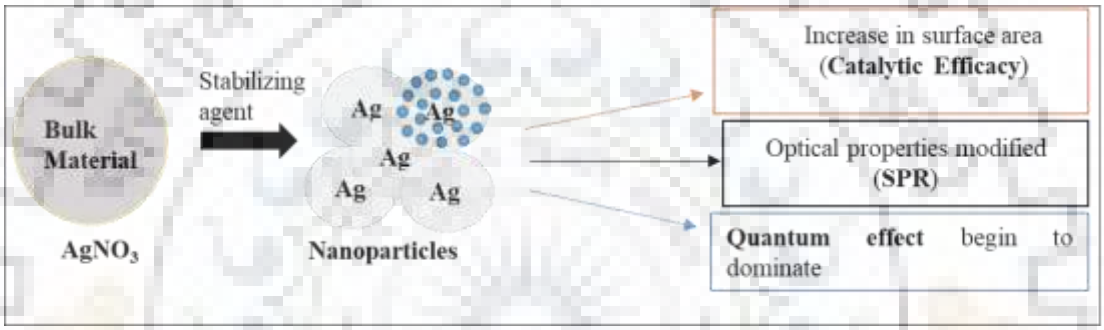

Figure 2.1: Modified properties of bulk materials in nanoparticle form.

This technology has transfigured various medical fields including immunology, pulmonology, endocrinology, ophthalmology, cardiology, oncology, etc. Also, they showed controlled release and are efficiently being utilized in the targeted tissue delivery [19, 20].

Nanoparticles are divided basically into two groups namely: organic and inorganic nanoparticles [21]. The organic group includes dendrimers, micelles, liposomes, and polymeric nanoparticles. The inorganic group includes quantum dots, fullerenes, silica, metal silver, gold, zinc oxide nanoparticles [22]. Currently, nanomaterials are being used in the food packaging industry that plays an essential role in improving the shelf life of food products by imparting anti-microbial mechanism. They are also being used in cosmetic products, wound dressings, drug delivery applications, and wastewater treatment applications [23]. Various leading cosmetic brands are employing nano-emulsions, liposomes, and other nanomaterials because of their enhanced solubility, transparency, and deeper skin penetration properties.

An additional property of these nanomaterials to protect skin from UV has also been explored by cosmetic companies to use them in sun-screen cream formulations [24] and have promising roles in bio-imaging applications such as molecular probes and bio-labels [25]. All these applications are based on their exclusive properties which are related to their small size.

Table 2.1: Potential applications of nanomaterials in different sectors.

Sectors	Applications	References
Biomedical	Wound dressing, Antibacterial creams, Drug delivery, Control release and Diagnostics	[16, 17]
Food Industry	Food packaging	[18]
Cosmetics	Sun screens	[19]
Environment	Wastewater treatment,	[20, 21]
	Environment catalysts	[22]
Power/ energy	Dye sensitized solar cells	[23]

2.2. Properties of nanoparticles

Functional behaviour and the applicability of nanomaterials in the biomedical applications is highly dependent on their morphological and chemical properties. Hence, minute modification at the chemical level such as their surface fabrication or replacement may result in impaired performance **(Fig. 2.1)** [20].

2.2.1 Shape and size

Shape and size are the most important properties of nanoparticles and influence their efficiency in various applications. Therefore, optimization of the size of nanoparticles is being done by various researchers for their application-oriented purposes e.g. Biomedical field. In biomedical applications, particles having size 0.1 µm to 7 µm can be detected by reticulum endothelium system in liver or spleen while those having less than 5 nm may suffer from glomerular filtration [33]. The shape of nanomaterial is directly correlated to their shape features like aspect ratio, convexity, solidity, and circularity [34]. These also play a major role in terms of functional properties of nanoparticles e.g. catalysis [35].

2.2.2 Optical properties

Metallic nanomaterials and nanocomposites show property of linear absorption, nonlinear optical properties, and photoluminescence emission. Nanomaterials with small particle sizes are efficient in providing enhanced optical emission and exhibit nonlinear optical properties owing to their quantum confinement effect [36]. Surface Plasmon Resonance (SPR) is an exclusive phenomenon shown by metallic NPs due to which they exhibit a wide range of colors by absorbing visible light [25].

2.2.3 Surface properties

Nanoparticles possess net electrical potential on their surface called zeta potential. It is the potential of a particle or molecule due to its charge in a certain medium that sometimes may impart the nanoparticles with a tendency to aggregate. There is a linear relationship between the absolute value of surface electric potential and the repulsion between nanoparticles [37]. Nanomaterials with versatile properties possess tremendous scope in the biomedical field. They have huge applicability in wound healing therapeutics owing to their catalytic efficiency and antimicrobial property [7, 15, 37].

2.3 Silver nanoparticles

Metallic NPs have already been explored to a great extent and have huge potential in nano-biotechnology. Silver nanoparticles possess excellent properties of conductivity, antimicrobial action, catalytic mechanism, and other size-dependent properties [38]. They possess huge potency to effectively interact with biomolecules in vivo and in vitro due to which they have high applicability in various diversified fields. Apart from biomedical applications, nanoparticles are proven to be efficient in wastewater treatment owing to their property of catalytic efficiency, mass transfer effect, and high surface area to volume ratio. Laser ablation, ultrasonic radiations, microwave radiations, and gamma radiation methods (physical methods), becoming popular these days due to their eco-friendly nature; regarded safe to be used in biomedical in-vivo applications because avoid using toxic chemicals. Various methods to synthesize silver nanoparticles [39] are, 1). Physical methods (Laser ablation, Microwave, Sonication), 2). Chemical methods ($NaBH_4$ (Sodium borohydride) reduction method)), 3). Biological (Microorganisms [40], Enzymes [41], Plant extract [42]). This study using Chemical reduction also known as “Brust-method” [24].

2.3.1 Applications of Silver nanoparticles

Silver nanoparticles containing wound dressings have a broad-spectrum effect against all bacteria and other microbes. Silver nanoparticles coated on polyethylene cloth are widely used in burn healing applications [44]. Biosensors have been developed to detect serum p53 in squamous cell carcinoma [45]. Studies on lung carcinoma have elucidated their role in the prevention of cancer and their potential applicability in chemotherapy and chemoprevention [46]. Bio-functionalized silver nanoparticles with a good affinity for DNA molecules are also gaining popularity in wound healing and cancer targeted gene therapy [47].

2.3.2 Antimicrobial activity of silver nanoparticles: Mode of action

Several research groups have reported that silver nanoparticles possess a multimode inhibitory action on microorganisms (**Fig. 2.2**) [48, 49].

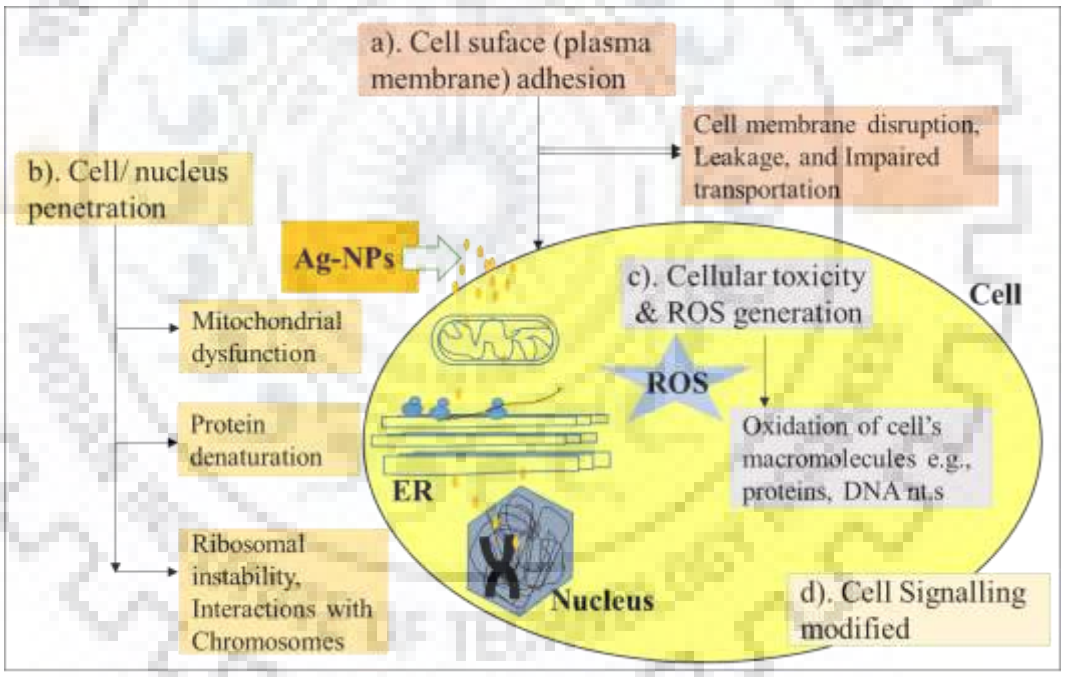

Figure 2.2: Multimode mechanism of action of silver nanoparticles over cells.

S.aureus is a gram-positive bacterium with an ability to produce mutli-layered biofilm embedded in a matrix comprising glycocalyx and proteins. *S.aureus* is the most commonly isolated bacteria in cases of diabetic open wounds (ulcers). *S.aureus* associated diseases include ocular infections such as conjunctivitis, endo-ophthalmitis and bone infections such as Osteomyelitis [25]. Gram-negative *P.aeruginosa* is commonly detected in nosocomial infections. These infections are associated with

catheterization and intubation [26]. Various types of antibiotics such as cell wall synthesis inhibitors (Glycopeptides, β- lactams), protein inhibitors (chloramphenicol, tetracyclines) and cell membrane disruptors (lipopeptides, polymyxins) are available which possess antimicrobial action against pathogens. However, the emergence of multidrug resistance and their tolerance to withstand antimicrobial agents has compelled the researchers to find novel solutions for better treatment. Metallic nanoparticles such as silver and gold have been widely studied for their antibacterial efficacy and possess huge potential in biomedical applications.

However, silver nanoparticles tend to aggregate in the absence of befitting capping agent. Therefore, biocompatible polymers with attractive physiological and biological properties are being employed to cap nanoparticles that have applicability in biomedical applications.

2.4 Assays for ROS detection:

a). Glutathione assay for redox status of the cell [27].

b). Fluorescent redox sensors e.g. 2, 7-Dichlorofluorescein (DCF), amplex red [28].

c). Chemiluminescent probes e.g. Luminol (HOCl), Lucigenenin ($ONOO^-$, O_2^-) [29].

2.5 PHAs

2.5.1 Resorbable medical scaffolding materials

Suture TephaFLEX® was the first ever approved product of PHB by FDA, pulmonary artery and valves made from combined polymer of polyglycolic acid (PGA) and PHB. PHB and PHBV (PHAs) are hydrophobic, piezoelectric biopolymers, thermo-processable, biocompatible, crystalline, and linear polyesters **(Fig.2.3)** in nature, therefore, can be utilized as drug carriers as microcapsules and nanoparticles [6, 55]. Known green methods to synthesize coated or uncoated Ag NPs are microwave, hydrothermal, nano-precipitation, solvent displacement, ink-jet, LASER and photo-reduction. By utilizing green methods various researcher in the field already synthesizes both PHB nanoparticles i.e. with and without metal. The anticancer drugs like doxorubicin can be filled inside the nanoparticle cavity and are found to be excellent carriers of drugs delivery and have shown controlled release. Magnetic Fe_3O_4 nanoparticles of PHB were formed using co-precipitation [56-66].

2.6 Common characterization techniques employed in this study

2.6.1 DLS and zeta potential

Basic principle of dynamic light scattering (DLS) is based on Brownian movements in colloidal solutions, and was related to Strokes-Einstein equation, which is having a component of drift velocity divided by the applied force, to calculate mobility of colloidal particles. Hydrodynamic size thus can be calculated based on interacting ion layers with nanoparticles and when laser beam showing diffraction of light in all possible directions, either interfere constructively or destructively forming the light and dark regions respectively [67].

Nanoparticle's charged surface attracts oppositely charged ions to form a thin layer over its surface. Zeta potential is the net potential that exists at the slipping plan or the plane of hydrodynamic shear. Zeta potential of beyond ±30 mV values is for stable colloids [37].

2.6.2 Microscopic and spectroscopic techniques

Versatile types of microscopic and spectroscopic techniques have been employed in various biomedical fields such as nano-biotechnology, microbiology, and biochemistry which have enabled the researchers to study detailed morphology dependent functional features of bio and nanomaterials. Microscopic techniques are broadly classified into optical and electron microscopy and the resolution is inversely related to wavelength. Electron microscopic techniques are SEM and TEM, which utilize high-intensity electron beam to capture images in nano-range. SEM is a technique to record the image of nanomaterials by targeting focused electron beam onto their surface. When this electron beam interacts with the sample, they reflect secondary and backscattered electrons with different kinetic energies that are detected by the detector. TEM operates on the same principle. However, the detector detects transmitted electrons in the case of TEM [68]. Fluorescence microscopy is an optical microscopic technique which is commonly employed in the bio-medicinal field. When a high intensity light is subjected on the sample, they undergo an excitation process followed by emission of florescent light as they decay from their excited state. Fluorophores are excited by a higher frequency light and emit a lower frequency light which is detected to produce images [69]. SPM e.g. AFM are beneficial to study surface characteristics such as roughness and adherence of nanomaterial on the surface.

Fourier transform Infrared (FTIR) spectroscopy technique is used to determine molecular fingerprint of the structure. When the sample is subjected to infrared radiation exposure, some amount of radiation is absorbed by the sample while the sample transmits the remaining one. Every bond or functional group requires different frequency for absorption [70]. This technique is highly beneficial to study the interaction between various compounds at a molecular level. Various characterization techniques have enabled the researchers to study detailed morphological, functional, and biological features of the nanomaterials. Therefore, they are being studied widely for their applicability in the medicinal field. The current study employs various microscopic, spectroscopic and other techniques to study structural and physicochemical properties of PHB-Ag NPs.

Chapter 3

Materials and Methods

3.1 Synthesis of encapsulated Ag-NPs by chemical reduction ($NaBH_4$) method

PHB and PHBV biopolymers were provided by **Dr. Saugata Hazra** lab (Biotechnology, IIT Roorkee), biosynthesized from waste using various bacterial species e.g. C1R. Silver nitrate ($AgNO_3$) was purchased from Sisco research laboratories Pvt. Ltd. stored in dark at 4 °C in a refrigerator.

3.1.1 Chemical synthesis of PHB-Ag NPs

PHB capped silver nanoparticles were synthesized using $NaBH_4$ Chemical reduction approach: PHB encapsulated silver nanoparticles (PHB-Silver NPs) were chemically synthesized instantly by mixing 19.5 µL of 5 mM $AgNO_3$ solution in distilled water with 0.8 mg PHB/ mL water (0.08 wt%) on a magnetic stirrer for 20 min. Abruptly adding 32 mM $NaBH_4$ (19.5 µL) stored in ice. Further, the reaction was carried out, for 10 minutes at room temperature on a magnetic stirrer @700 rpm, so that all the reactants can be consumed in the process.

3.1.2 Chemical synthesis of PHBV-Ag NPs

The PHBV encapsulated silver NPs were also synthesized and optimized using $NaBH_4$ Chemical reduction: PHBV film was dissolved in miliQ overnight on a magnetic stirrer at 80 ^oC and silver nanoparticles (PHB-Ag NPs) were encapsulated by mixing 19.5 µL of 5 mM $AgNO_3$ solution in DW with 0.8 mg PHBV in 1 mL water (0.08 wt%) on a magnetic stirrer. Abruptly adding 32 mM $NaBH_4$ (10 µL) stored in ice. The color of the solution was then became yellow confirms formation of encapsulated silver nanoparticles. The color of Ag-NPs was due to “Surface Plasmon Resonance” effect after absorption of visible light.

3.2 Characterization of PHB and PHBV encapsulated Ag NPs

3.2.1 UV/Vis spectroscopy

The synthesized Ag NPs solutions were first analysed and characterized by The Eppendorf Bio Spectrometer using a single beam scan in 250 nm- 600 nm range. Single, high-intensity absorption peak around 400 nm confirms Ag NPs formation in solution. The basic principle of absorption in visible light is Surface plasmon resonance effect of nanoparticles.

3.2.2 DLS and Zeta Potential (mV)

The freshly synthesized PHB or PHBV-Ag NPs (hydrodynamic size) were analysed using Nano series Zs ZETA sizer, Malvern Instrument. The Hydrodynamic size (using Strokes and Einstein equation for colloidal particles undergoing Brownian motion) and Zeta potential (the potential at slipping plane or plane of hydrodynamic shear) of respective Nanoparticles were supportive for further characterizations since the colloidal stability were found to be good enough that NPs will not agglomerate but no information for the shape of nanoparticles at this stage.

3.2.3 FE-SEM analysis

Scanning Electron Microscope (Carl Zeiss FE-SEM, Germany) was utilized to image the detailed sample morphology and composition (EDX) PHB and PHBV-Ag NPs.

3.2.4 High-resolution TEM analysis

The nano dimensions of the synthesized PHB-Ag NPs were investigated by recording TEM images using high-resolution transmission electron microscope. Each nanoparticle separately did on a C- coated Cu grid by adding one drop of nanoparticles solution and the solvent was dried in red light. Images of PHB- or PHBV-Ag NPs dried on the C-coated Cu-grid were captured in TEM. Size distributions of nanoparticles were determined using ImageJ software. One limitation of the TEM is that it requires very thin specimens, otherwise, the electrons are strongly scattered within the specimen, or even absorbed rather than transmitted. SAED (selected area electron diffraction) and energy dispersive X-rays analysis patterns of respective nanoparticles were also recorded.

3.2.5 FTIR analysis

FTIR spectroscopy analysis of capped nanoparticle solutions was carried out to determine functional groups involved in the synthesis and stabilized PHB-Ag NPs and PHBV-Ag NPs. FTIR (Thermo Nicolet nexus) was used for spectra of 4000–400 cm^{-1}.

3.2.6 XRD analysis (Small Angle/Thin-Film X-Ray Diffractometer)

X-ray diffraction (Thin film coating) is a technique utilized to characterize the crystallographic features in the sample, using Cu as a target. Freshly prepared PHB-Ag NPs and PHBV-Ag NPs were made consecutive thin layers on glass slide substrates. They were air dried overnight, Further, analysed in X-ray diffractometer (D8 advance,

Bruker and miniflex, Rigaku). The angle range of 10-90° with 0.01°/min scan. Leptos and EVA software used for measurement and analysis.

3.2.7 TGA/DTA analysis

Freshly prepared samples of PHB-Ag NPs and PHBV-Ag NPs were lyophilized at -80 °C and scanned in N_2 atmosphere in the 0 ºC to 800ºC of the temperature range. Furthermore, DTA, DTG and TGA spectra were recorded on the same sample with the help of a precision balance which measures the weight of the sample as a function of time.

3.2.8 FE-SEM (FEI) analysis

FE-SEM QUANTA 200 FEG (FEI Netherlands) was used for freshly prepared PHB and PHBV encapsulated Ag NPs and treated bacterial cell were analysed and images were recorded using FE-SEM to study morphological features of the coated Ag-Nanoparticles and treated cells.

3.2.9 SPM analysis

Integra (model NT-MDT) SPM was used for imaging and 3-D surface measuring, fine as much as a level of molecules or groups of atoms with extremely fine probe tips, and a flexible cantilever of very low spring constant.

3.3 Antimicrobial activity of PHVB encapsulated Ag NP solution

Culture of *S.aureus* in LB media was grown for 12 h at 37 °C, 190 rpm. The 12 h cultures were diluted with fresh LB 1:10 i.e., 2 µL culture was added to 20 µL fresh autoclaved LB. Cultures were treated with 50 µL of PHB-Ag NPs solution at 37 °C, 190 rpm for 9-10 h. Afterward, the antibacterial effect of the solution was evaluated by optical turbidity analysis at OD_{600}.

3.4 Antimicrobial activity of PHB encapsulated Ag NP solution

The treated culture at a concentration of 180 µg/mL of PHB-Ag NPs showing OD_{600} as 1.4 while MIC value for PHB-Ag NPs was found to be around 360 µg/mL, cultures showing no visible growths (0.136). Thus, OD_{600} of treated culture for *S.aureus* showed no increase in cell density which is very less in comparison to control (2.047). In the case of PHBV coated silver NPs the MIC value is the original concentration of NP solution i.e. 180 µg/mL, and the treated culture tube showed an OD_{600} value of 0.063.

3.5 Antimicrobial activity of coated-Ag NPs against bacterial strains

The study of the antibacterial effect of NPs was done using turbidity assay of broth culture and then, 96-well plate assay. Culture tubes were subsequently treated with different concentrations of PHB-Ag NPs and were incubated at 37 °C at 200 rpm for 8 h. The culture tube with the lowest OD after 8 h incubation period was considered as MIC value.

3.5.1 Determination of MIC of coated-Ag NP

MIC (Minimum inhibitory concentration) of may be defined as the minimum nanoparticle concentration that does not allow microbes to grow. Concentrated solution of LB (4x) was autoclaved and then diluted accordingly with autoclaved distilled water to see direct effects of nanoparticles solutions. The culture tube which was not showing a visible growth over 6 h incubation at 37 ^{o}C. Thus, In case of PHB coated NPs when used to treat *S.aureus* cells at a concentration of 360 µg/mL, the OD value at 600 nm was 0.136 which can be compared to their normal growth OD 2.049, implies no visible growth. This implies that MIC of PHB-Ag NPs against *S. aureus* is around 360 µg/mL.

3.5.2 Microtitre 96-well culture plate assay for MIC

LB media was prepared using 1 g LB/ 20mL D.W. and 100 µL was used for 96 well plate assay, added to each well. Ampicillin (0.1 mg/mL), 5 µL was added to column 3.

1. **Reference:** 100 µL Autoclaved DW + 100 µL Media 2x [LB].

2. **Control (-):** 100 µL Autoclaved DW + 100 µL Media 2x [LB] media + cells respectively.

3. **Ampicillin Control (+):** 100 µL Autoclaved DW + 100 µL Media 2x [LB] media, and add respective cells.

4. Add 100 µL 2x [LB] media to all remaining columns (wells).

5. Add PHB and PHBV-Ag nanoparticles 100, 50, 25, 12.5 µL (360 µg/mL) to A-D and E-G to 4, 5, 6, 7 columns and repeats 8, 9, 10, 11 columns respectively.

6. Add PHB and PHBV polymer solutions 100 µL A-D and E-G respectively to 12th column. Lastly add respective cells (2 µL),12 h incubate plate at 37 ^{o}C incubator.

3.5.3 Microscopy analysis

Bacterial cells were treated, harvested and washed with normal saline pH 5.5 to remove extra media moieties and fixed using 10 µL of 2.5% glutaraldehyde. Smear of culture was prepared on the glass slide and air dried for 1 h. Images of treated and untreated bacterial cultures were recorded using FE-SEM and SPM.

Chapter 4

Results and Discussion

4.1 UV-Vis spectroscopy

$AgNO_3$ and PHB alone have not shown any absorption peak. While the colored solution of PHB coated nanoparticles showing strong absorption at 403 nm **(Fig. 4.1a)** and in the case of PHBV-Ag NP, the UV-Vis absorption peak at 415 nm **(Fig. 4.2)**.

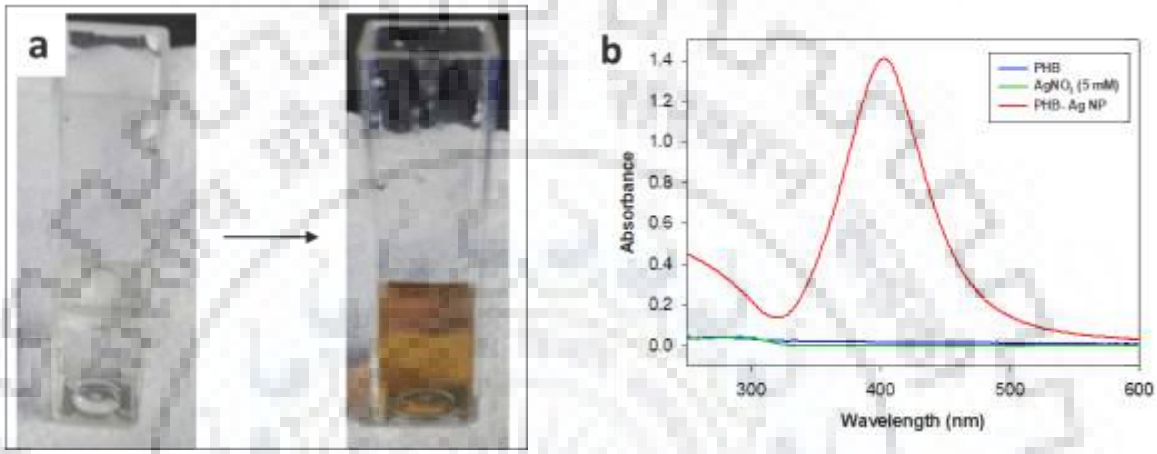

Figure 4.1: **a).** The color change of a solution to yellow indicating the formation of PHB-Ag NPs, **b).** Absorption (250-600 nm) spectra of PHB-Ag NPs.

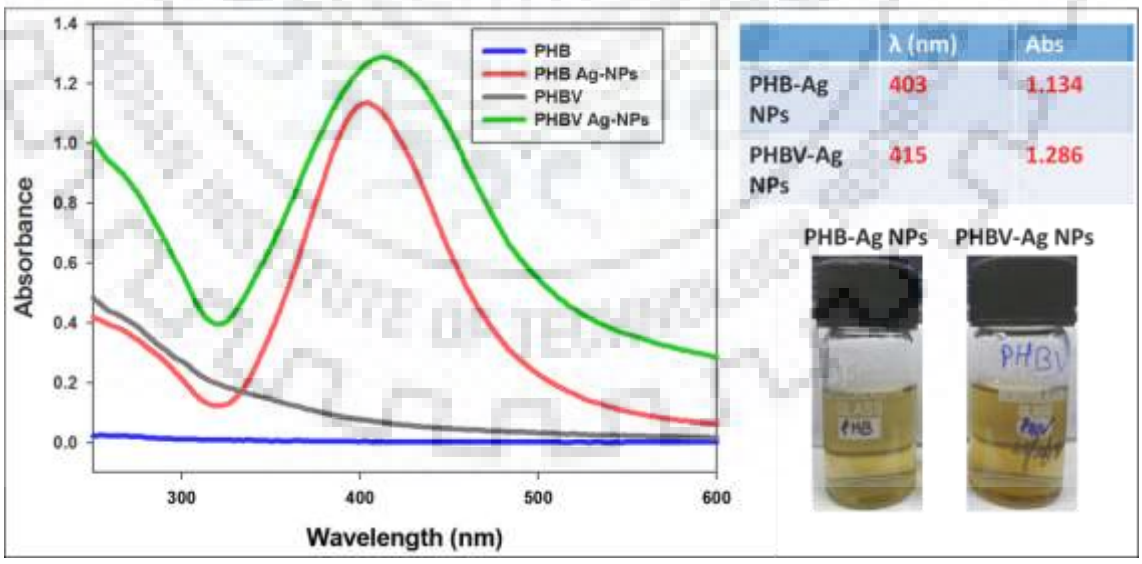

Figure 4.2: Relative absorption peak positions of PHB (blue), PHB-Ag NPs (red), PHBV (grey), PHBV-Ag NPs (green) and their relative intensities.

4.2 DLS and Zeta potential analysis

The PHB encapsulated silver NPs are was having an average hydrodynamic size of 120.7 nm with a polydispersity index (PDI) value of 0.376. **(Fig. 4.3a)**. While Z-average in case of PHBV-Ag NPs is 78.24 nm, having PDI of 0.264 **(Fig. 4.3b)**. In both the cases, the nano-size range distribution showing monodispersed nature of the nanoparticles.

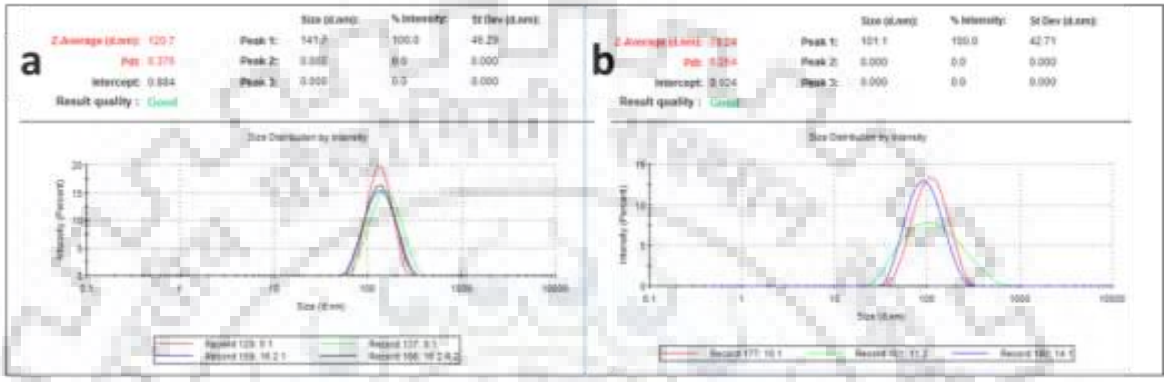

Figure 4.3: DLS hydrodynamic size measurement (Z-average (nm)), Polydispersity-index of **a)** PHB-Ag NPs, and **b)** PHBV-Ag NPs.

Zeta potential of -43 mV **(Fig. 4.4a)** for PHB-Ag NPs showed good colloidal stability and do not undergoes agglomeration in solution. Zeta potential value of PHBV encapsulated silver NPs was found to be -37.6 mV with long shelf-life and good colloidal stability **(Fig.4.4b)**. The negative charge over nanoparticles repel each other in the colloidal solution and thus, will not agglomerate. The PHB or PHBV stably coat the surfaces of silver nanoparticles as seen by TEM analysis of respective nanoparticles, and thus, are found to be good encapsulating agents for in vivo applications, since these biopolymers are biocompatible and biodegradable.

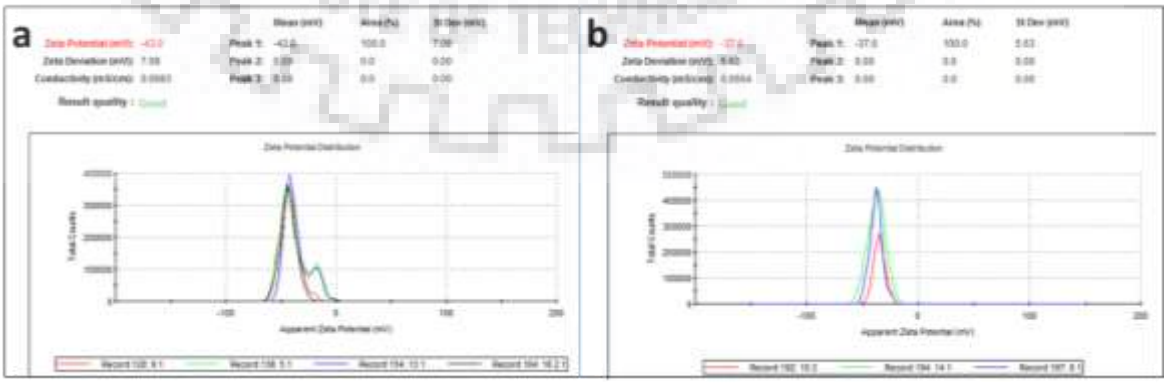

Figure 4.4: Zeta potential (mV) of **a)** PHB-Ag NPs, and **b)** PHBV-Ag NPs.

4.3 FTIR analysis

To see which functional groups are engaged and interacting with reduced silver atoms, to form stabilizing interactions, have to carry out FTIR **(Fig.4.5 and Fig. 4.6)**. The major relative shifts **(Table 4.1 and Table 4.2)** are summarized respectively for polymer and after the formation of coated silver nanoparticles.

Table 4.1: FTIR shifts: PHB vs PHB encapsulated silver nanoparticles.

PHB polymer	PHB-Ag Nanoparticles
887.17 cm^{-1}, 21.80%T	880.68 cm^{-1}, 27.5%T
1555.18 cm^{-1}, 7.75%T	1569.61 cm^{-1}, 10.49%T
2086.82 cm^{-1}, 16.13%T	2092.89 cm^{-1}, 22.82%T

Table 4.2: FTIR shifts: PHBV vs PHBV encapsulated silver nanoparticles.

PHBV polymer	PHBV-Ag Nanoparticles
666.17 cm^{-1}, 14.59%T	615.45 cm^{-1}, 11.2%T
1302.24 cm^{-1}, 16.25%T	1352.59 cm^{-1}, 13.95%T
1638.02 cm^{-1}, 4.91%T	1631.38 cm^{-1}, 3.72%T
2081.97 cm^{-1}, 16.50%T	2089. cm^{-1}, 22.82%T

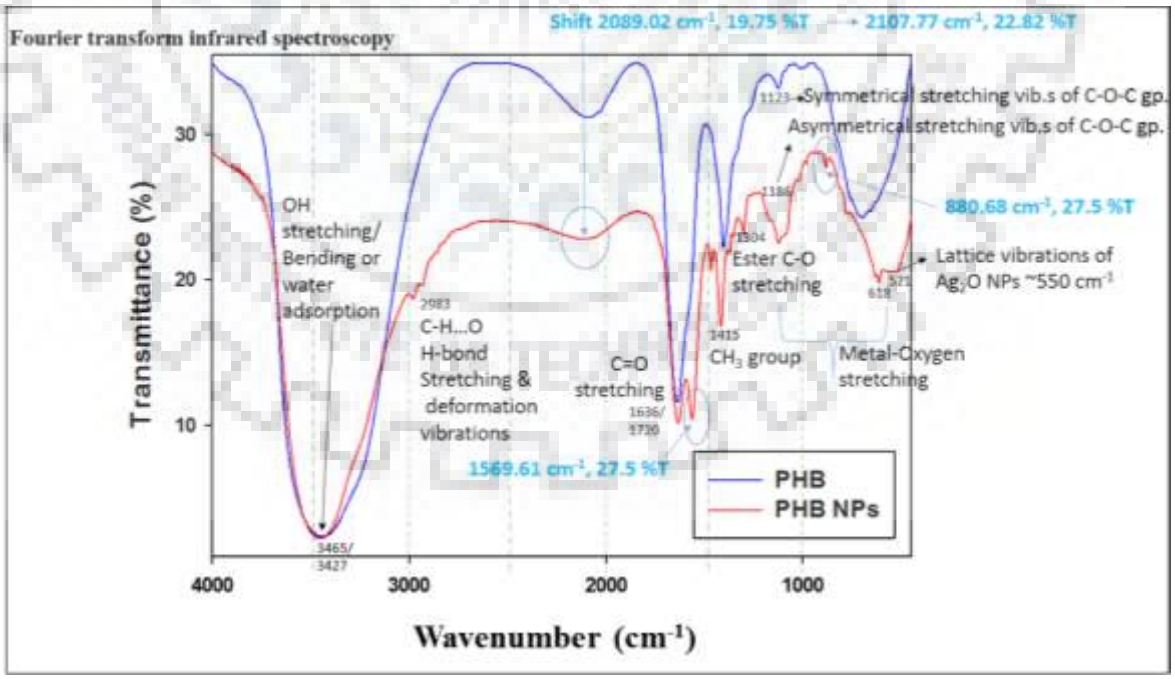

Figure 4.5: FTIR spectra of PHB polymer (blue), and PHB-Ag NPs (red).

Main characteristic peak of PHB and PHBV solutions is the new peak of C=O stretching emerged due to Ag NP at 1554 cm^{-1}. Strong bend at 1121 cm^{-1} showed C-O-C stretch, C-O-H bending vibrations of PHB or PHBV polymers when interacts with charged silver atoms. Similar shifts and new peaks are observed in the case of PHBV NPs and PHB NPs, which when compared with their respective polymer's solution alone, confirms the formation of PHBV encapsulated Ag-NPs. FTIR spectra also confirm the formation of Ag_2O NPs stretch ~550 cm^{-1}. The carboxylate, carbonyl, and hydroxyl groups are showing involvement in interacting with reduced silver.

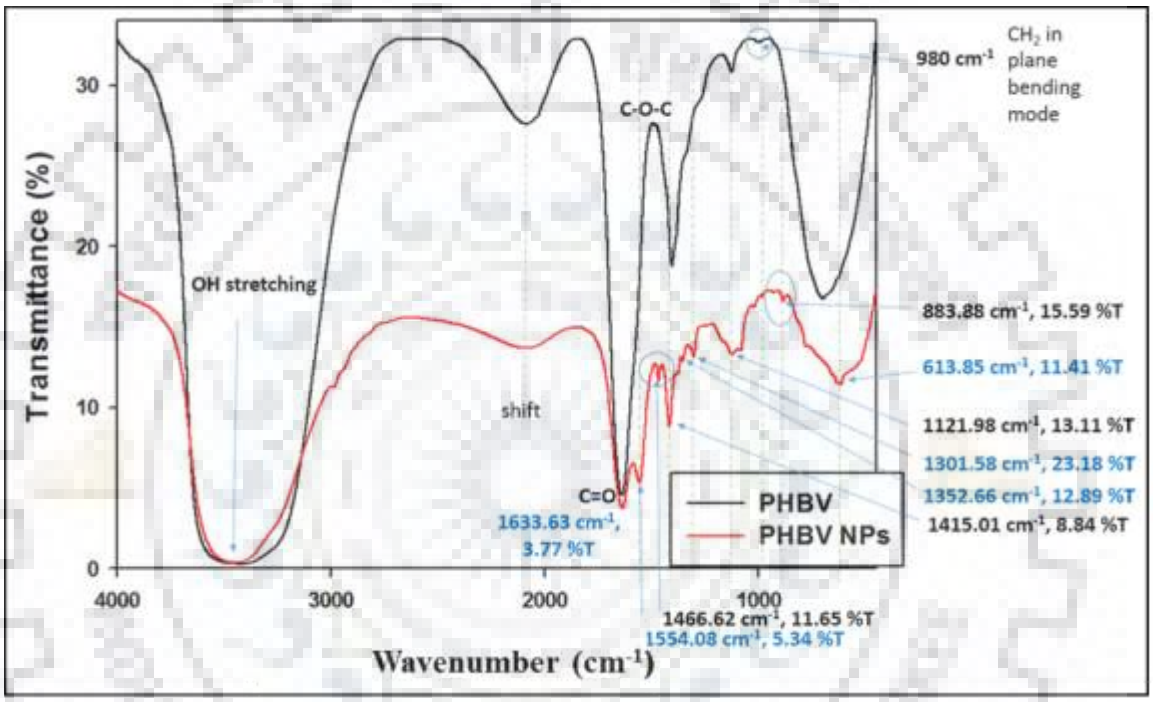

Figure 4.6: FTIR spectra of PHBV polymer (black), PHBV-Ag NPs (red).

4.4 Electron microscopy analysis

4.4.1 Scanning electron microscopy of PHB-Ag NPs

Field Emission-Scanning electron micrograph at 100 nm resolution and an applied voltage of 20 KV of PHBV-Ag NPs showed monodispersed NPs in nano-size range. FE-SEM micrograph of PHB-Ag NPs showed plenty of separately seated nanoparticles in nano-range **(Fig. 4.7a)**. TEM images **(Fig. 4.7b and Fig. 4.7c)** also depicted the spherical and oval shapes of encapsulated Ag NPs at 20 nm. The nano-coatings of biopolymers PHB and PHBV can be more precisely seen in TEM images **(Fig. 4.7c)**. The resultant average nanoparticle diameter of PHB coated Ag NPs was calculated to be 12.5±2 nm, NP size distribution 8 nm to 20 nm range **(Fig. 4.9a).**

4.4.2 Scanning electron microscopy of PHBV-Ag NPs

Field Emission-Scanning electron micrograph at 100 nm resolution and an applied voltage of 20 KV of PHBV-Ag NPs showed monodispersed NPs in nano-size range. It also depicted the morphology of encapsulated Ag-NPs **(Fig. 4.8)**. ImageJ software analysis was done to calculate the average nanoparticle diameter **(Fig. 4.9)**. The resultant average nanoparticle diameter of PHB coated Ag NPs was calculated to be 12.5±2 nm, NP size distribution 8 nm to 20 nm **(Fig. 4.9a)**, On the other hand the PHBV-Ag NPs are smaller in size (5.1±1nm), showed 2 nm to 7.5 nm size range **(Fig. 4.9b)**.

4.4.3 TEM analysis

TEM images showed the coating over of silver nanoparticles to form stabilized PHB encapsulated silver NPs approximately 8-20 nm under 50 nm scale **(Fig. 4.10)**. Spherical shape of PHB-Ag NPs was observed at 20 nm scale **(Fig. 4.7c)**. EDX showed 3.66% of silver signals for aqueous solution of PHB encapsulated silver NPs which implies the formation of Ag NPs and coating of the polymer **(Fig. 4.11a)**.

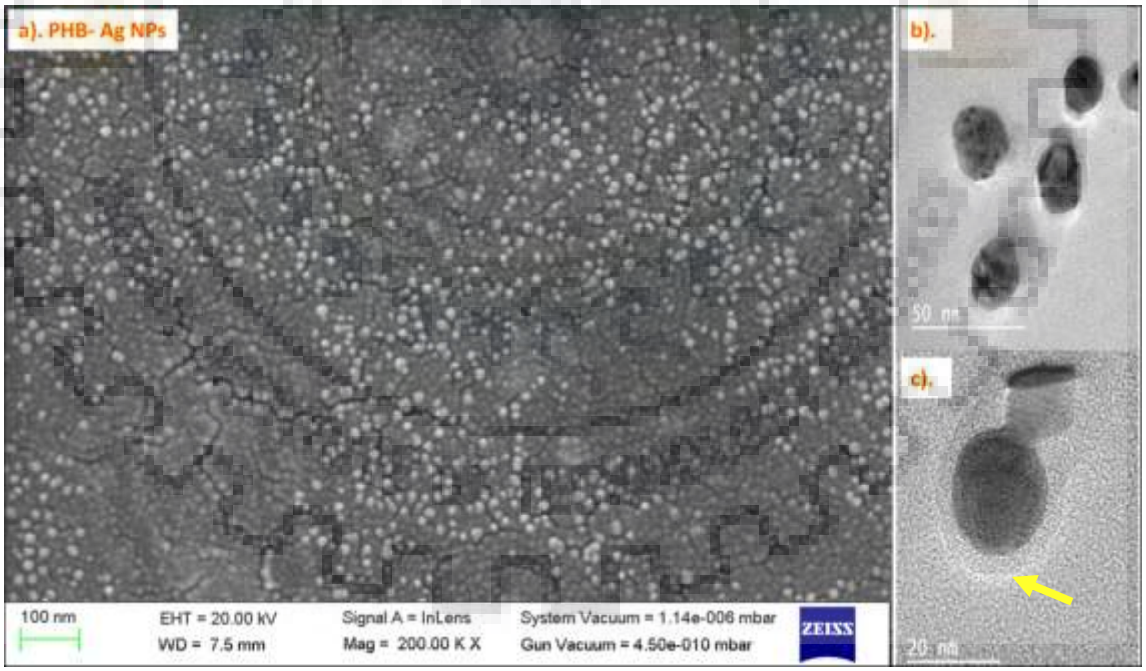

Figure 4.7: Electron Microscopy images of PHB-silver NPs **a)** SEM image: PHB-silver NPs, **b)** TEM image: PHB-silver NPs at 50 nm scale, and **c)** TEM image of PHB-silver NPs at 20 nm scale showing PHB encapsulation over silver NPs (arrowhead).

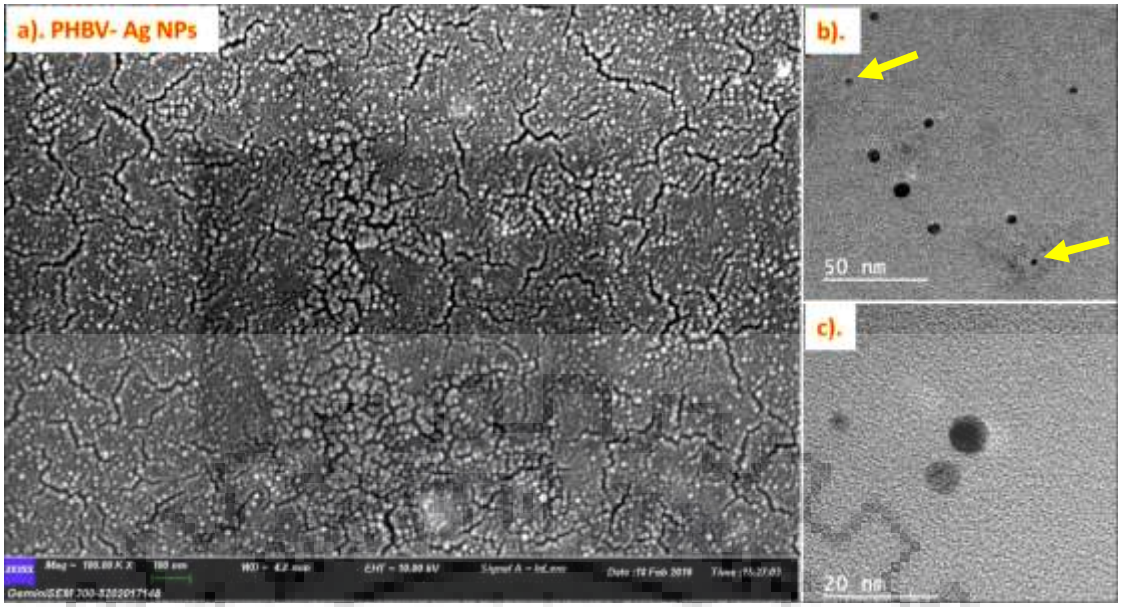

Figure 4.8: Electron Microscopy images of PHBV-Ag NPs **a)** SEM image of PHBV-silver NPs, TEM image **b)** PHBV-Ag NPs at 50 nm scale, and **c)** PHBV-Ag NPs at 20 nm scale.

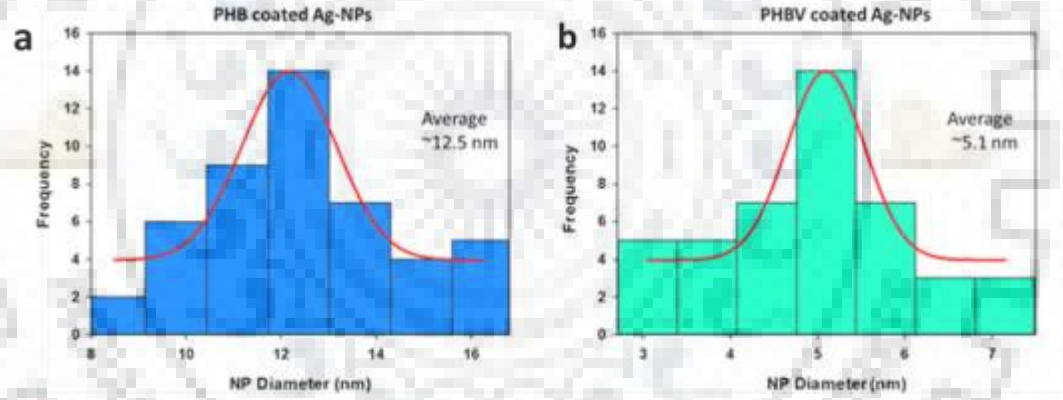

Figure 4.9: ImageJ average size analysis **a)** PHB-Ag NPs and **b)** PHBV-Ag NPs.

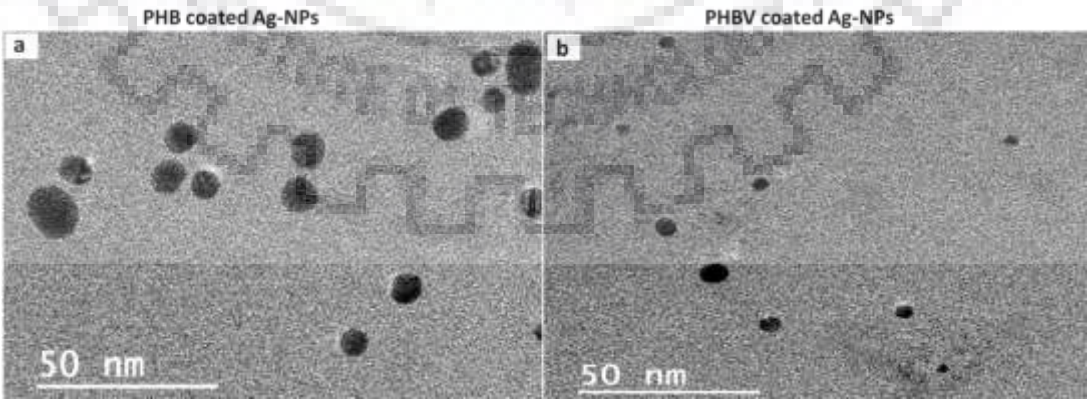

Figure 4.10: TEM image of **a)** PHB-Ag NPs, and **b)** PHBV-Ag NPs at 50 nm scale.

EDX spectrum of PHBV Ag NPs showed 1.58% of silver signals for aqueous solution of PHBV-Ag NPs **(Fig. 4.8c)** which implies the formation of PHBV-Ag NPs

(Fig. 4.11b). Selected area electron diffraction **(**SAED) pattern was found to be poly-nanocrystalline (small spots making up rings, each spot arising from the individual crystallite's Bragg reflection) as seen in the case of PHBV coated Ag NPs. Selected area (electron) diffraction diffused rings may be attributed to amorphous carbon film **(Fig. 4.12)**.

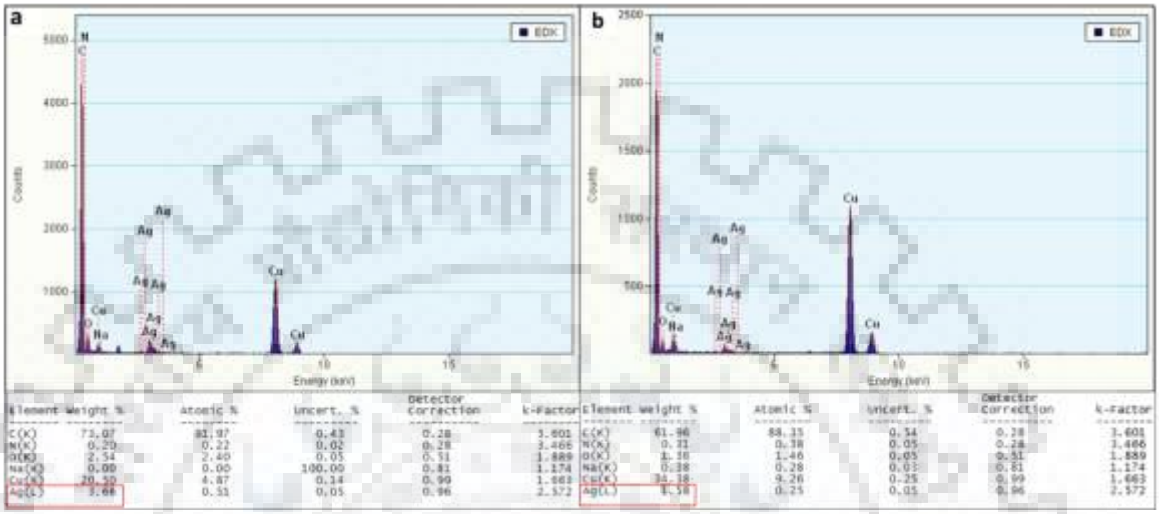

Figure 4.11: TEM- EDX pattern of **a)** PHB-Ag NPs, and **b)** PHBV-Ag NPs.

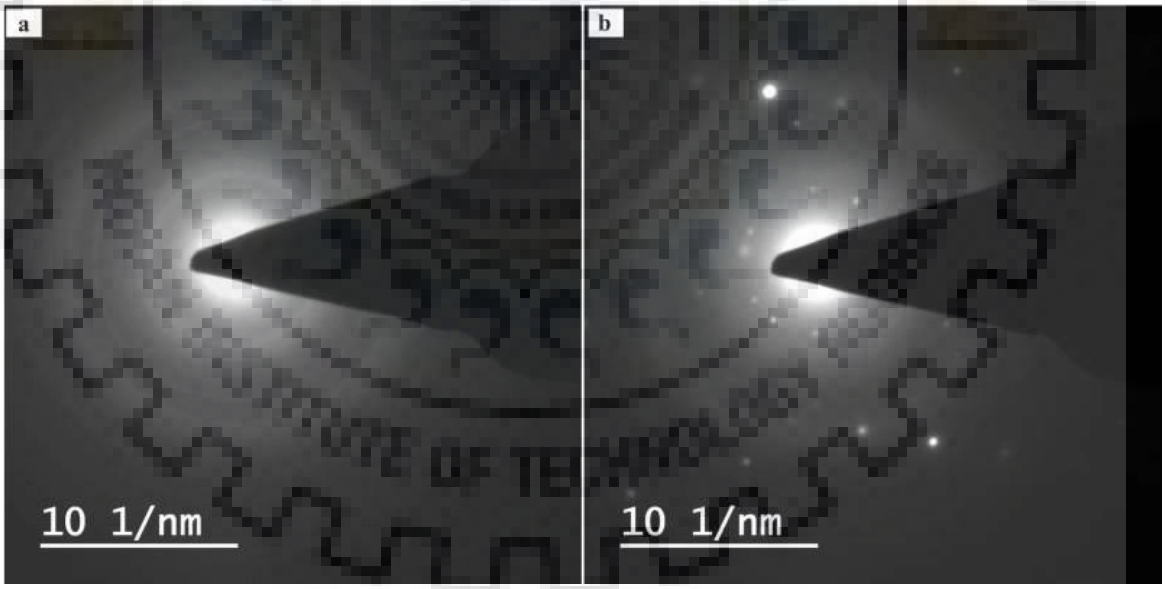

Figure 4.12: TEM- SAED pattern of **a)** PHB-Ag NPs, and **b)** PHBV-Ag NPs.

4.5 SPM analysis

SPM includes AFM, and STM used to analyze the 3-D surface morphology, roughness, structure of nanomaterials. The average roughness was found to be 2.99 nm and 3.30 nm respectively in case of PHB-Ag NPs and PHBV-Ag NPs **(Fig. 4.13)**.

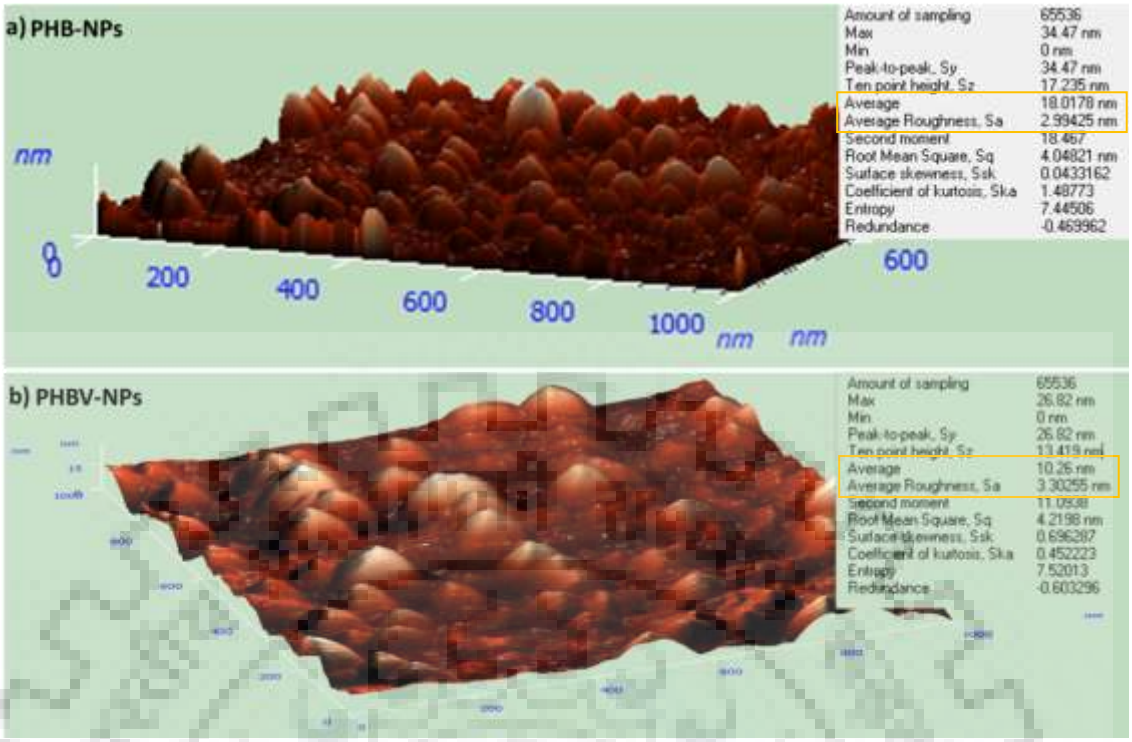

Figure 4.13: SPM 3-D analysis of **a)** PHB-Ag NPs, and **b)** PHBV-Ag NPs.

4.6 XRD analysis

XRD thin film data showing the planes of PHB capped nanoparticles (PHB-Ag NPs) depicted their crystalline nature. No crystal planes were seen in the case of PHB polymer alone. Sharp crystalline reflections at 37°, 42°, 64°, 72°, and 76.5° and ~ 80° are showing encapsulated silver NP's (111), (200), (220), (311), and (331) planes of FCC crystal structure **(Fig. 4.14)**. Peaks in PHB-Ag NP exactly matches the silver atoms (JCPDS file number 04-0783) in FCC structure.

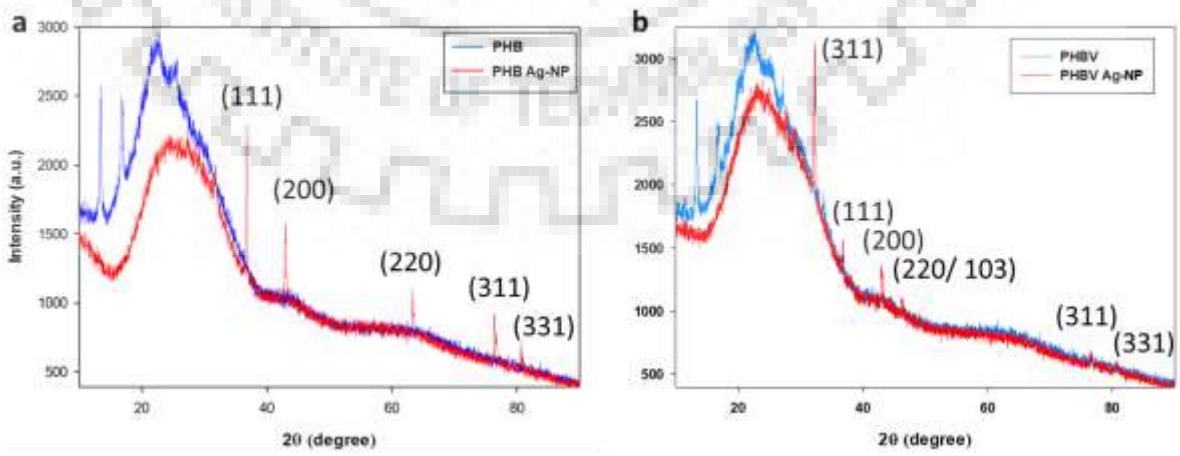

Figure 4.14: XRD patterns PHB-Ag NPs compared with PHBV Ag NPs.

4.7 TGA/DTA analysis

Thermogravimetric analysis (TGA) is the method of thermal changes (increase in temperature) correlated with the decrease in mass of the sample in a controlled atmosphere (N_2 gas). Thus, we can see encapsulated Ag-NPs are more thermally stable than polymer alone. TGA analysis can also be used for thermal, oxidative stability or sample compositional studies. On the other hand, DTA (differential thermal analysis), and Differential Thermogravimetric (DTG) measures wt. loss in the sample during the heating procedure. In the case of PHB polymer the mass loss of polymer started at 219 ^{o}C (97.5%) and continues till 265 (-1.1%) and all the polymer has consumed in this temperature range **(Fig. 4.16a)**. While in the case of capped PHB-Ag-NPs **(Fig. 4.16b)**, withstand up to 247 ^{o}C (98.9%) and even at 289 ^{o}C, 0.1% coated sample remained which was consumed at higher temperatures in the process of thermal oxidation **(Fig. 4.15** and **Fig. 4.16)**.

The pink peak showed 259 ^{o}C (50.1%/min) vs 285 ^{o}C (73.1%/min) for DTG analysis of PHB polymer and PHB-Ag NPs (**Fig. 4.15a** and **Fig. 4.15b**). The green small peak showed 175 ^{o}C, 14.32 µV (58.2 µV.s/mg) and large (green) peak 260 ^{o}C, 1.30 µV (819 µV.s/mg), vs 175 ^{o}C, 12.77 µV (50.9 µV.s/mg) and 286 ^{o}C, 2.81 µV (404 µV.s/mg) for DTA analysis of PHB polymer and PHB-Ag NPs respectively (**Fig. 4.15a** and **Fig. 4.15b**). While, the blue peaks are TGA data of PHB vs PHB-Ag NPs are compared in a better way (**Fig. 4.16**).

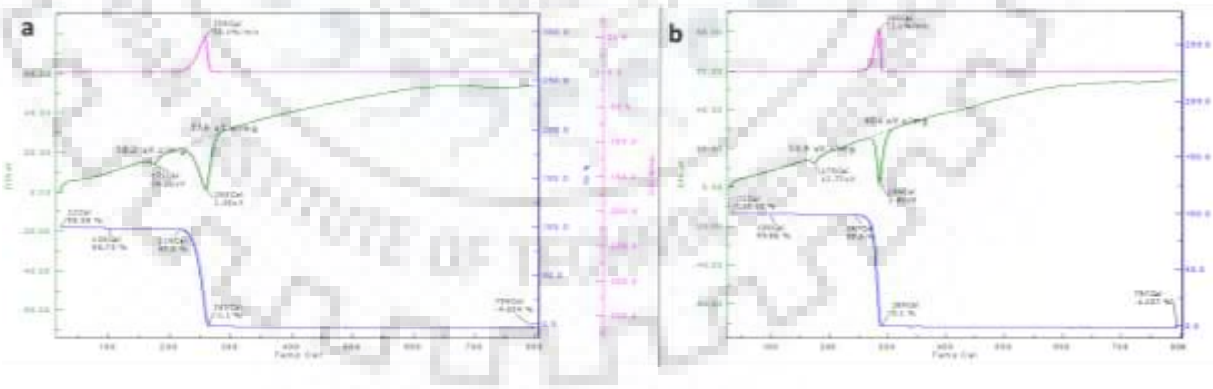

Figure 4.15: TGA/DTA analysis of **a)** PHB polymer, and **b)** PHB-Ag NPs.

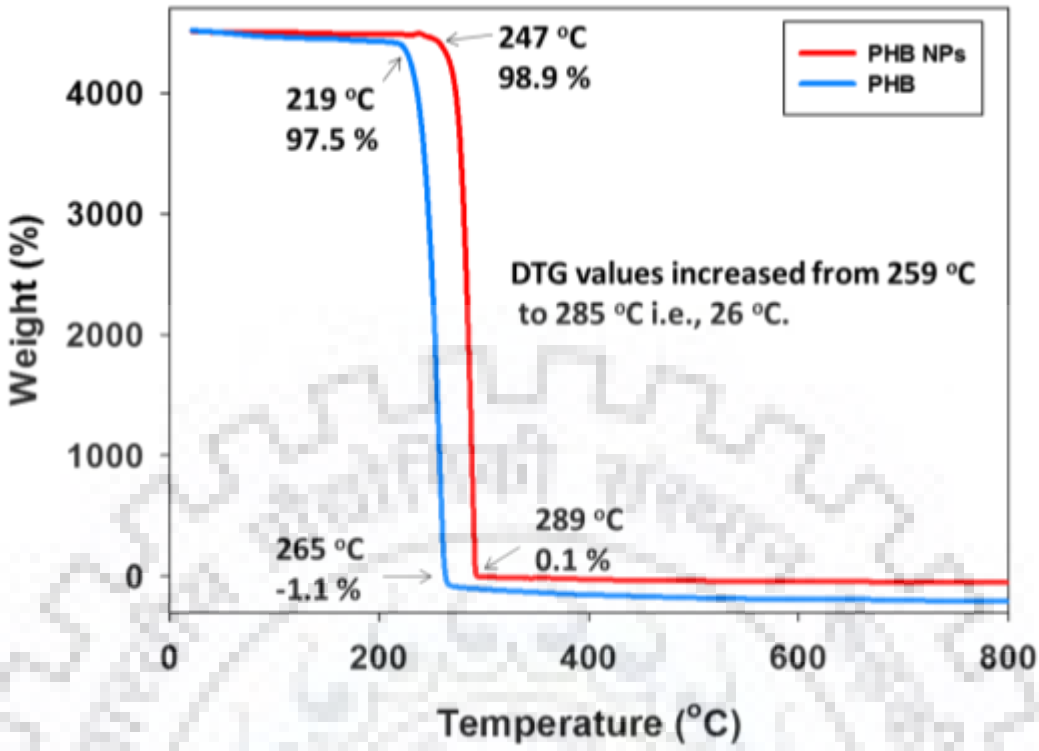

Figure 4.16: TGA analysis of **a)** PHB polymer (blue), and **b)** PHB-Ag NPs (red).

4.8 Antimicrobial activity

The treated culture at a concentration of 180 µg/mL of PHB-Ag NPs showing OD_{600} as 1.4 while MIC value for PHB-Ag NPs was found to be around 360 µg/mL, cultures showing no visible growths (0.136) **(Fig. 4.17)**. Thus, OD_{600} of treated culture for *S.aureus* showed no increase in cell density which is very less in comparison to control (2.047). In case of PHBV coated silver NPs the MIC value is the original concentration of NP solution i.e., 180 µg/mL, and the treated culture tube showed an OD_{600} value of 0.063. The Growth kinetics of PHBV treated *S.aureus* was also studied **(Fig. 4.18)**.

PHBV encapsulated Ag-NPs are found to be more potent anti-bacterial at less nanoparticle concentrations, since they are only 1/3rd in diameter than PHB coated Ag-NPs **(Figure 4.20 and Fig. 4.21)**.

4.9 Antimicrobial assay

Encapsulated-Ag nanoparticles are bacteriostatic, and bactericidal as can be seen by SEM and broad-spectrum antimicrobials. MIC may be defined as the nanoparticles concentrations which does not allow microbial growth in treated cultures overnight.

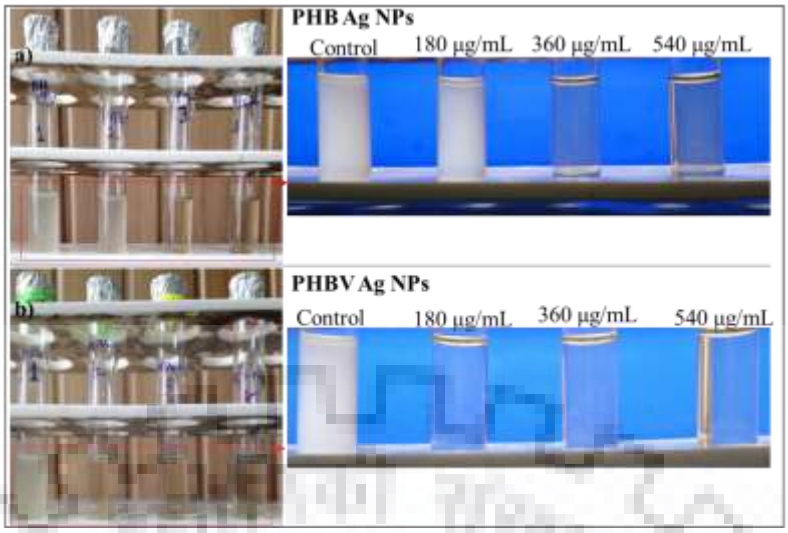

Figure 4.17: Turbidity assay showing comparative antimicrobial action of PHB-Ag NPs against PHBV-Ag NPs for *S.aureus*.

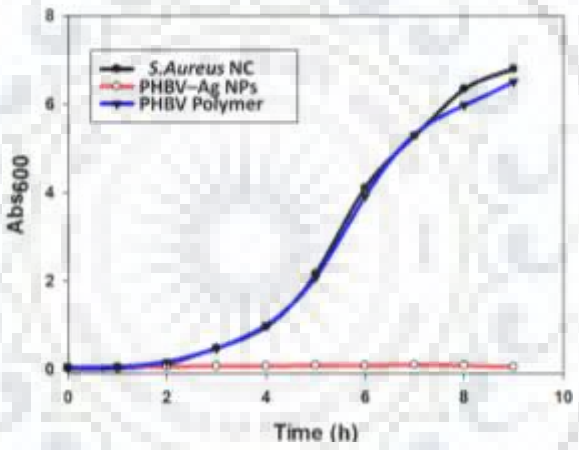

Figure 4.18: Growth Kinetics of *Staphylococcus aureus*: i). Black sigmoid curve is normal growth (negative control), ii). Blue curve in presence of polymer alone, and iii). Red curve showing treated culture with PHBV-Ag NPs.

Table 4.3: OD_{600} showing PHBV, PHBV encapsulated silver nanoparticles treated *P.aeruginosa.*

Time	Negative control	Positive control	PHBV solution	PHBV-Ag NPs (µg/mL)	
				360	720
0 h	0.009	0.033	0.038	0.107	0.178
12 h	0.008	0.968	0.991	0.112	0.180
36 h	0	1.019	0.953	0.979	0.174

This may also suggest that they did not allow growth of other microorganisms too by bacteriostatic or bactericidal mechanisms. Microtitre-plate assay by seeing absorbance at 600 nm depicting antimicrobial activity of encapsulated-silver NPs (3-PHB, PHBV) against i) *E. coli,* ii) *P.aeruginosa,* iii) *S.aureus* and iv) *Bacillus thuringiensis* **(Fig. 4.20)**.

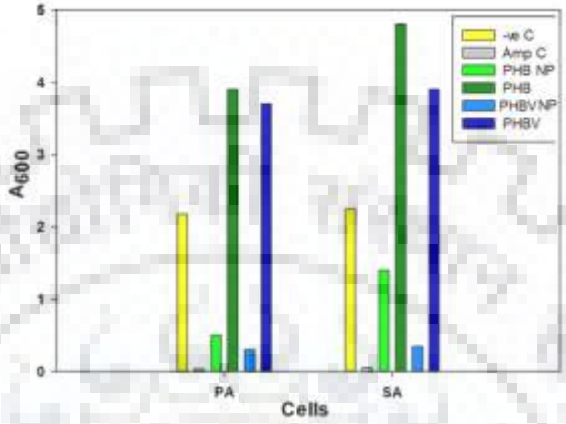

Figure 4.19: 96 well-plate assay of encapsulated-Ag NPs (PHB, PHBV) against **a)** *P.aeruginosa,* **b)** *S.aureus.*

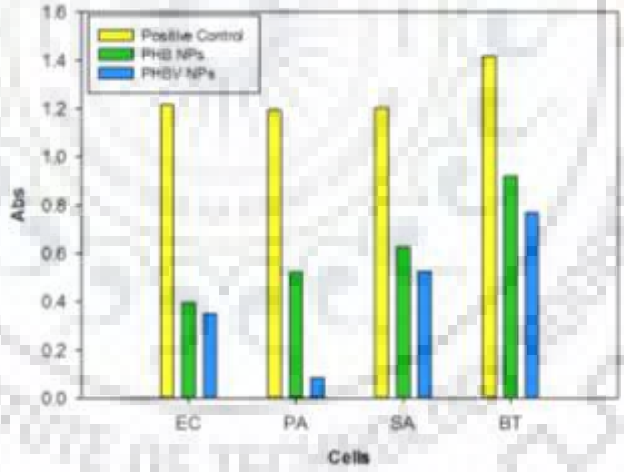

Figure 4.20: 96 well-plate assay absorbance at 600 nm depicting antimicrobial activity of encapsulated-Ag NPs (PHB, PHBV) against *E.coli, P.aeruginosa, S.aureus, and B.thuringiensis.*

MIC via 96-well plate assay in which single colonies of above-mentioned strains were first inoculated in 2 mL fresh LB and incubated for 12 h at 190 rpm. Then, turbid cultures were diluted using fresh LB, so that, each culture tube contains approximately 8 X 10^5 CFU/mL. Culture tubes were subsequently treated with different concentrations of PHB-Ag NPs, and were incubated at overnight at 200 rpm.

PHB- or PHBV-Ag NPs treated *S.aureus* and untreated *S.aureus* was subjected to SPM and FE-SEM analysis **(Fig. 4.21** and **Fig. 4.23)**. Untreated *S.aureus* **(Fig. 4.21a)** showed smooth morphology of the bacterial cell colonies, On the other hand, PHB-silver NPs and PHBV-silver NPs treated *S.aureus* **(Fig. 4.21b and Fig. 4.21c)** showed lysis of PM and release of cellular contents. The binding of PHB-Ag NPs on the bacterial outer membranes and ultimately leads to the internalization of PHB-Ag NPs. PHB-Ag NPs or PHBV-Ag NPs treated *P.aeruginosa* and untreated *P.aeruginosa* was subjected to SPM **(Fig. 4.22)** and FE-SEM analysis **(Fig. 4.24)**. Untreated *P.aeruginosa* **(Fig. 4.24a)** showed smooth morphology of the bacterial cells, On the other hand, PHB-silver NPs and PHBV-silver NPs treated *P.aeruginosa cells* showed lysis of PM and release of cellular showed broken and ruptured cells **(Fig. 4.22b and Fig. 4.22c)**.

4.10 Agar Disc-diffusion assay (Kirby-Bauer antibiotic testing)

Relative antibacterial activity of PHBV-silver NPs over PHB-silver NPs can be seen using Kirby-Bauer assay. ZOI are of the diameter for Gram positive *S.aureus* was about14±1 mm vs 12±1 mm and for Gram negative strain *P.aeruginosa* were of diameter about12±1 mm vs 10±1 mm **(Table 4.4)** of 360 µg/mL PHBV-silver NPs and PHB-silver NPs respectively. The ZOI of capped silver NPs is directly proportional to their concentration.

4.11 SEM and EDX analysis to observe cell lysis

Antimicrobial property of coated NPs may be attributed to bactericidal or bacteriostatic mechanism and was demonstrated using broth method, micro-culture plate assay, and finally the lysed cells were seen and confirmed by using microscopy approaches. Culture of *S.aureus* in LB media were 12 h, 37 °C, and 190 rpm.

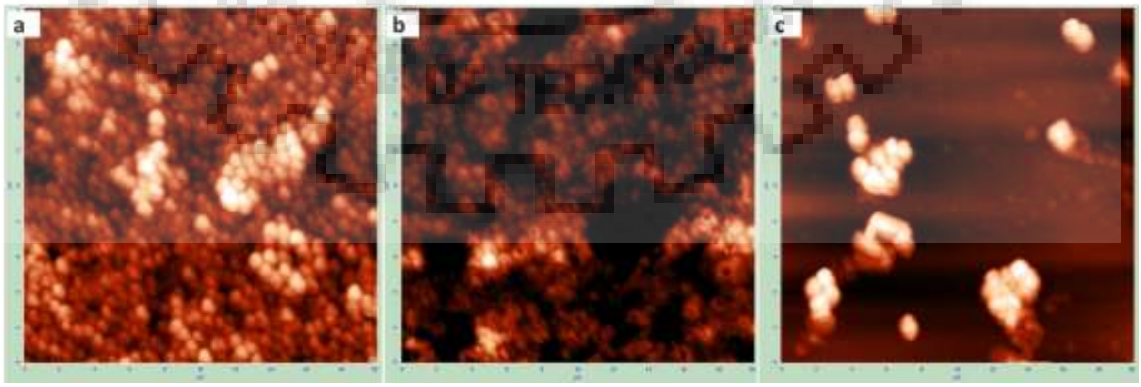

Figure 4.21: SPM depicting antimicrobial activity against *S.aureus* of **a)**. Negative control (NC), **b)**. PHB-Ag NPs, **c)**. PHBV-Ag NPs.

Bacterial cells were treated, harvested and washed with normal saline pH 5.5 to remove

extra media moieties and fixed using 10 µL of 2.5% glutaraldehyde. Smear of culture was prepared on the glass slide and air dried for 1 h. Images of treated and untreated bacterial cultures were recorded using FE-SEM and SPM.

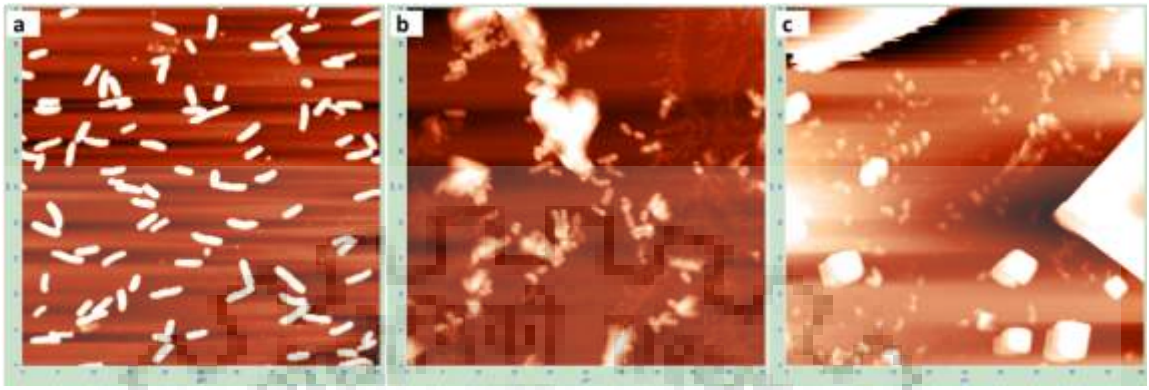

Figure 4.22: SPM depicting antimicrobial activity against *P.aeruginosa* of **a)**. Negative control (NC), **b)**. PHB-Ag NPs, **c)**. PHBV-Ag NPs.

The turbid cultures were diluted with fresh LB 1:10 i.e., 2 µL culture was added to 20 µL fresh autoclaved LB. Cultures were treated with 50 µL of PHB-Ag NPs solution and incubated at, 190 rpm, 37 °C for 10 h. Now, the antibacterial effect of the solution was evaluated by optical turbidity analysis at OD_{600}.

Table 4.4: Antibacterial efficacy of coated-silver NPs against *P.aeruginosa* and *S.aureus.*

Antimicrobial agent	**Concentrations (in µg/mL)**	**Inhibitory zone diameter (in mm)**	
		***P.aeruginosa* (Gram –ve)**	***S.aureus* (Gram +ve)**
Ampicillin (1)	1000	16±2	40±2
PHBV-Ag NPs (2)	360	12±1	14±1
PHB-Ag NPs (3)	360	10±1	12±1

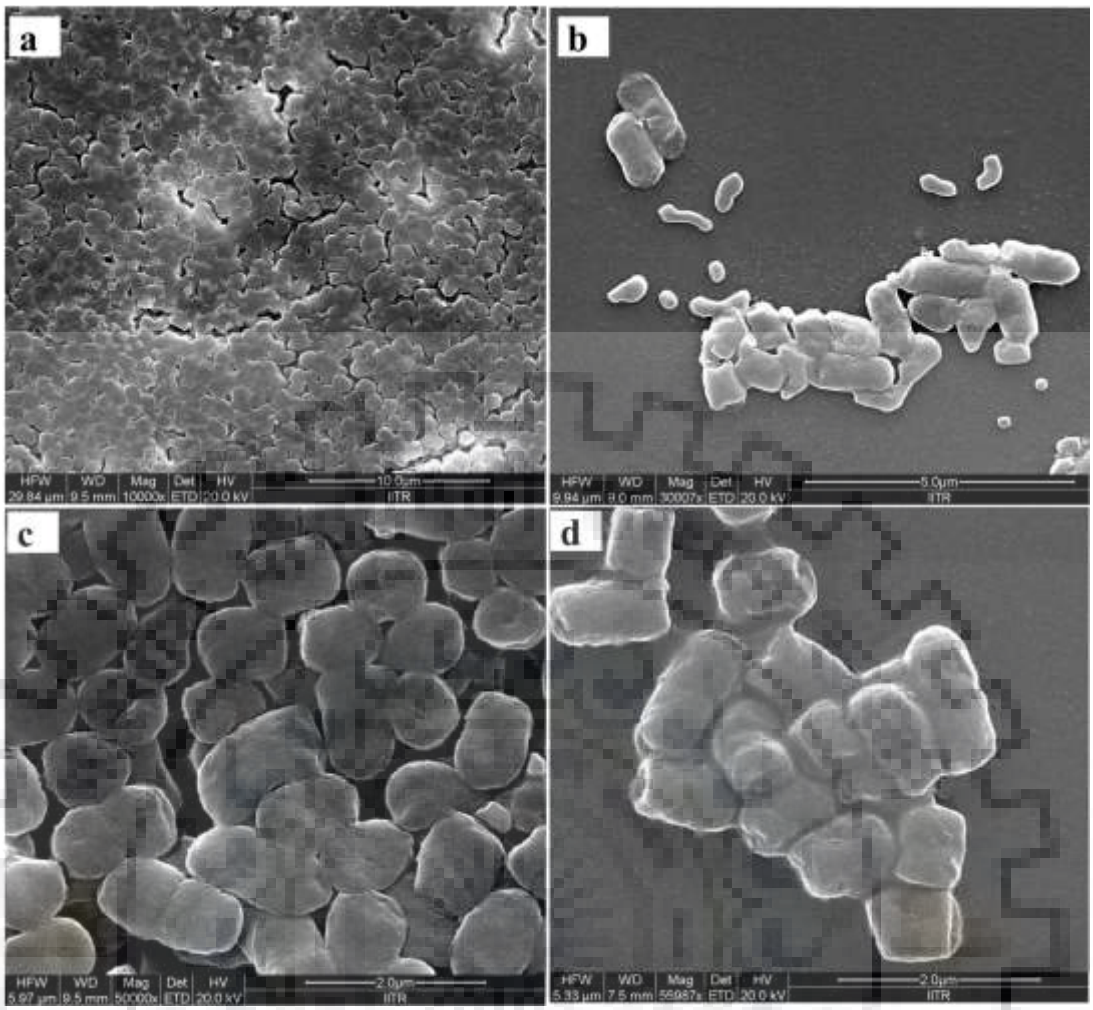

Figure 4.23: SEM images of *E. coli* untreated (**a, c**), treated with PHBV-Ag NPs (**b, d**).

4.11.1 Cell preparations for microscopy:

Cultures of treated *E.coli, P.aeruginosa, S.aureus, B.thuringiensis,* and *S.epidermidis* were grown at body normal temperature (37 °C), 190 rpm 12 h in LB. Then, they were diluted in using fresh LB medium (1: 100) and 360 µg/mL concentration of PHBV Ag NPs.

PHBV-silver NPs were added to treat the cells for 6-8 h. Cells were centrifuged and pellet was washed with normal saline pH 5.5 to remove extra media moieties and fixed using 10 µL of 2.5% glutaraldehyde. Smear of culture was prepared by pouring a drop (20 µL) of culture on the glass slide and air dried for 1 h. Encapsulated-Ag NPs treated *E.coli* **(Figure 4.23)**, *P.aeruginosa* **(Figure 4.24)**, *S.aureus* **(Figure 4.25)**, *B.thuringiensis* **(Figure 4.26)**, and *S.epidermidis* **(Figure 4.27)** were subjected to FE-SEM analysis. Images of treated and untreated bacterial cultures were recorded using FE-SEM and SPM.

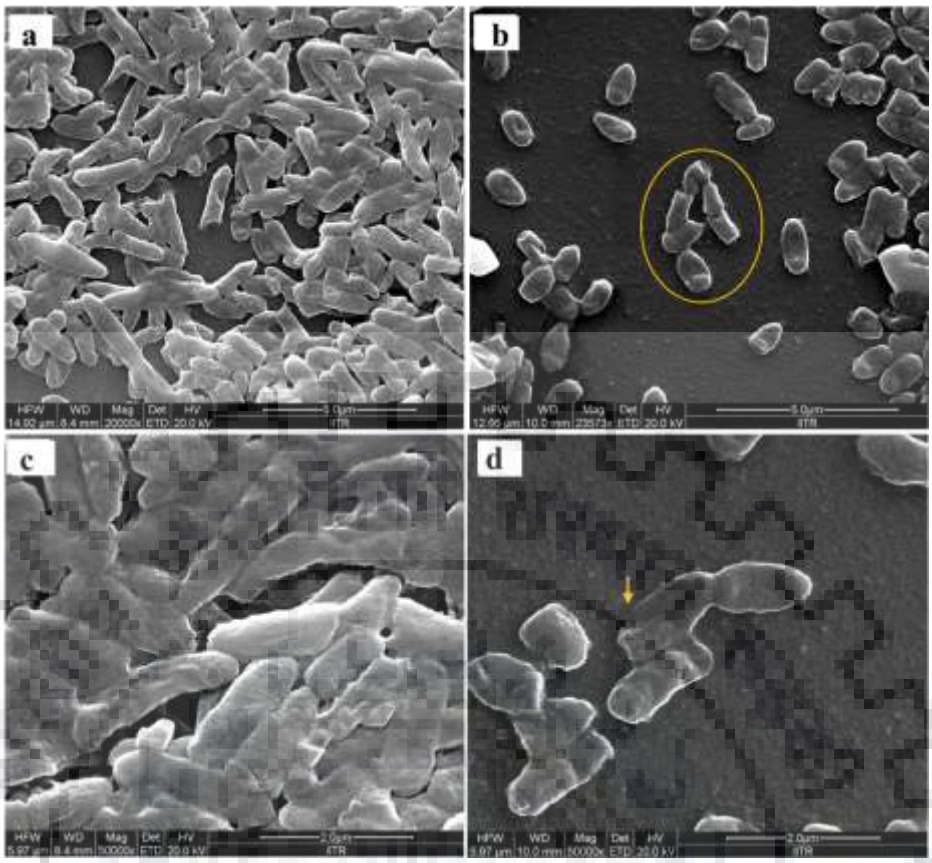

Figure 4.24: Images of SEM without treatment (Normal) *P.aeruginosa* cells (**a, c**), treated cells with PHBV-Ag NPs (**b, d**). Ruptured and broken cells are highlighted.

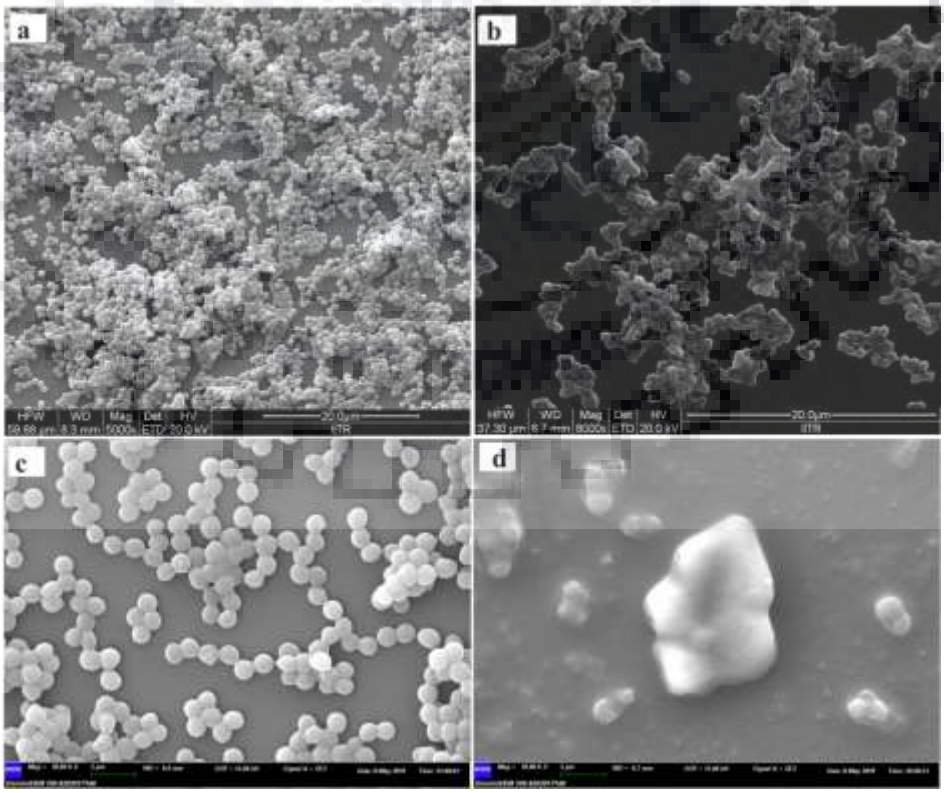

Figure 4.25: SEM of normal *S.aureus* cells (**a, c**), PHBV-Ag NPs treated cells (**b, d**).

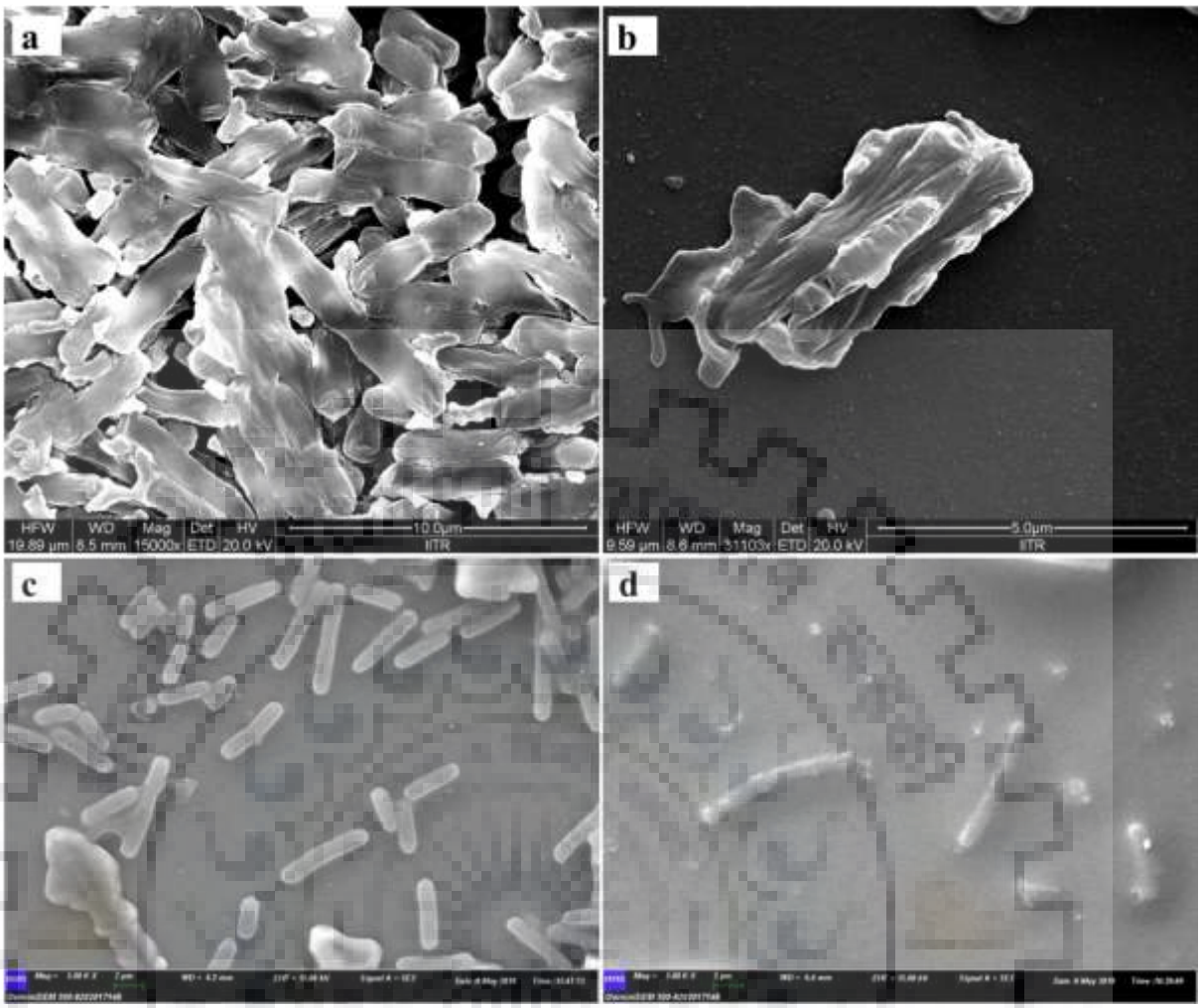

Figure 4.26: SEM images of *Bacillus thuringiensis* untreated (**a, c**), treated with PHBV-Ag NPs (**b, d**).

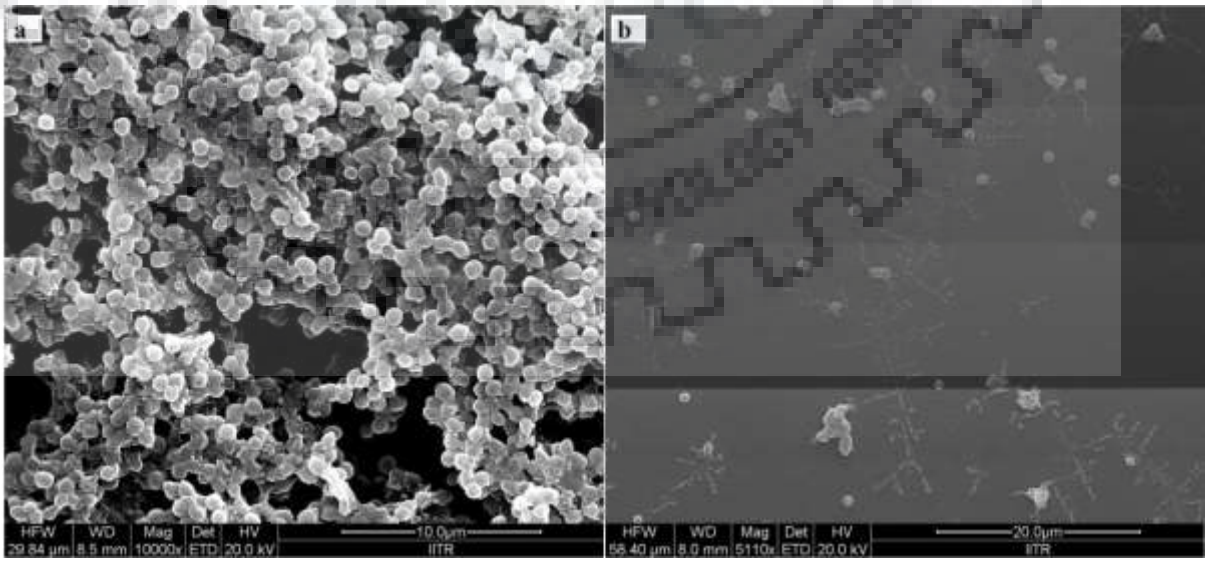

Figure 4.27: SEM images of *Staphylococcus epidermidis* untreated (**a**), and treated with PHBV-Ag NPs (**b**).

4.11.2 SEM- EDX analysis

Polymer coated silver NPs were added to treat the cells for 6-8 h. Cells were centrifuged and the pellet was washed with normal saline pH 5.5 to remove extra media moieties and fixed using 10 µL of 2.5% glutaraldehyde. A smear of culture was prepared by pouring a drop (10 µL) of culture on the glass slide and air dried for 1 h. Encapsulated-Ag NPs treated *S.aureus* **(Figure 4.25)** were subjected to FE-SEM analysis. EDX spectra recorded on the surface of treated cells also depicted the role of silver nanoparticles in rupturing the bacterial outer membrane and cell lysis **(Figure 4.28)**. The damaged morphology of PHB- or PHBV- Ag NPs treated bacterial cells can be attributed to the binding of coated Ag NPs on the bacterial outer membranes and ultimately the internalization of antimicrobial and bactericidal Ag NPs, leads to cell's lysis upon treatment at inhibitory concentrations.

Element	Weight%	Atomic%
O K	61.09	74.03
Na K	28.59	24.11
Ag L	10.32	1.86
Totals	100.00	

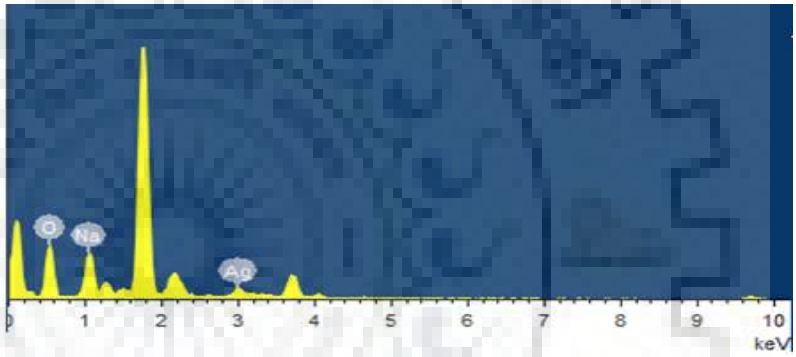

Figure 4.28: EDX spectra showing PHBV-coated silver nanoparticles treated bacterial cells.

4.12 Anti-cancer assay

A549 human alveolar adenocarcinoma cells, developed in 1972 by D.J. Giard, who isolated them from the tissue of lung cancer (male). MTT (light sensitive tetrazolium dye) dye reacts with mitochondrial reductase (NADPH- dependent dehydrogenase) to form an insoluble formazan (purple). Highly metabolically active cells reduce more dye. So, MTS assay is a colorimetric proliferation assay, gives an absorption maximum at 490 nm in PBS. 15 µL of original nanoparticle solution i.e., both PHB or PHBV encapsulated Ag nanoparticles showed almost neutral effects when compared to the negative control **(Figure 4.29c)**. The effects of original concentrations of PHB and PHBV nanoparticles are seen on A549 adenocarcinoma cells of human at 5 µL, 10 µL, and 15 µL volume concentrations, which were in the case of antimicrobials

are effective enough to inhibit bacterial growths but showing no such effects in case of cancerous cells.

4.12.1 MTS Assay for A549 cancer cell line

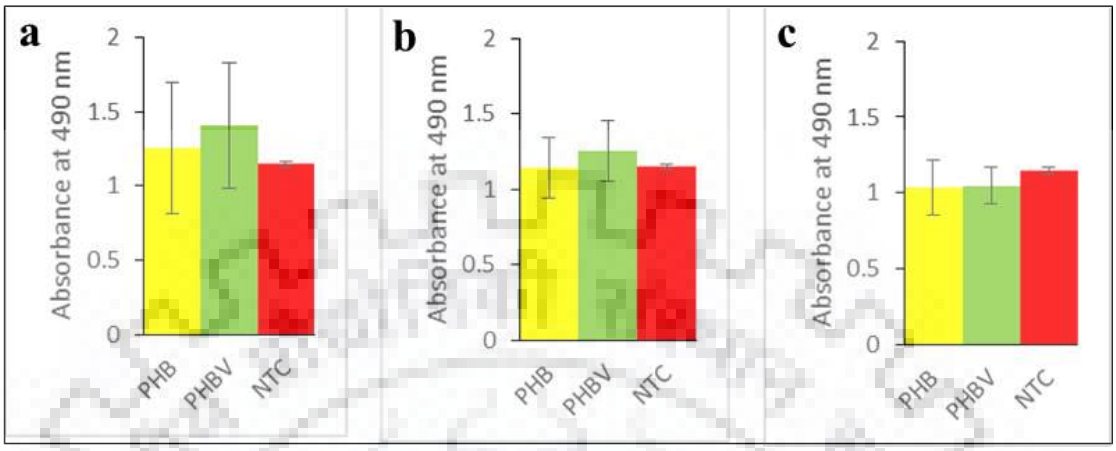

Figure 4.29: Anticancer effects of PHB-Ag NPs (yellow), PHBV-Ag NPs (green), negative (NTC) control (red) at original concentrations **a)**. At 5 µL **b)**. 10 µL and **c)**. 15 µL.

Chapter 5

Concluding Remarks and Future Perspectives

5.1 Concluding Remarks

In short, this report is about the instant chemical reduction of $AgNO_3$ and synthesis of PHB or PHBV (green renewable biodegradable biopolymers) encapsulated silver nanoparticles without using any toxic surfactants. Polyhydroxyalkonates e.g. PHB and PHBV used in this study are green, renewable bioplastics that can stably encapsulate Ag atoms from $AgNO_3$ by simple chemical reduction synthesis method using $NaBH_4$ as a reducing agent. The method described is found to be effective, simple, and instant. Synthesized nanoparticles are very small in size (2-25 nm) with very good stability in original colloidal solution form (zeta potential ~ 40 mV). These nanoparticles have been found to be efficiently removing *S.aureus, B.thuringiensis*, *P.aeruginosa, E.coli,* and *S.epidermidis* bacterial species and further intervention may possibly lead to the revelation of their potential as antibacterial therapeutics against biofilms. PHBV-Ag NPs are found to be more effective antibacterial agents due to their smaller size than PHB-Ag NPs, and, having better nano-characteristics e.g. surface roughness.

Possible Applications

(1). **In medicine**: Human blood contains PHB monomers as a normal non-toxic metabolite. Within blood and mammalian tissues, PHB is biocompatible & it is biodegradable too. Our Body can reabsorb PHAs, might be beneficial in surgical implants, surgery, and sutures. (2). **In pharmacology**, as microcapsules of PHAs as gene and drug packaging material. (3). **Packaging** in the industry of packaged food, like bottles, coating or sprayed foils for fast foods, and fibers.

Owing to GRAS status, biocompatibility and biodegradability of PHB, it can be used to enhance the antibiotic abilities of the silver nanoparticles. Hence this study legitimately provides assurance that the PHB encapsulated silver NPs holds a great promise in this novel antimicrobial field for biomedical applications, e.g. antimicrobial, antifouling coatings of food packets and dressing applied to the wounds to suppress infections at sites of open injury.

Limitations: PHAs are costly and thermally unstable during processing, therefore,

need to prepare nanocomposites/ blends to improve thermal and mechanical properties.

5.2 Future Perspectives

- ✓ Comparative analysis of polyhydroxyalkonates (PHAs) e.g. PHV and their composites for the antimicrobial properties.
- ✓ Though chemical synthesis is fast, required very low concentrations of reactants, but still, need to find some green synthesis alternatives of biopolymer encapsulated nanoparticles.
- ✓ Evaluation of PHB or PHBV encapsulated Ag NPs for their ability to act as antifungal agents to explore their biomedical applications in detail e.g. in food packaging and wound dressing.
- ✓ To make composites and blends of PHB, PHBV or both to further improve their thermal, mechanical properties and their applications.
- ✓ To work further on functionalization of PHB or PHBV encapsulated Ag NPs to be applicable in vivo applications, also require highly pure biopolymers.

References

1. Singh S, Singh SK, Chowdhury I, Singh RJTomj. Understanding the mechanism of bacterial biofilms resistance to antimicrobial agents. 2017;11:53.
2. Goel A, Meher MK, Gupta P, Gulati K, Pruthi V, Poluri KMJCp. Microwave assisted κ-carrageenan capped silver nanocomposites for eradication of bacterial biofilms. 2019;206:854-62.
3. Dicker MP, Duckworth PF, Baker AB, Francois G, Hazzard MK, Weaver PMJCpAas, et al. Green composites: A review of material attributes and complementary applications. 2014;56:280-9.
4. Shrivastav A, Kim H-Y, Kim Y-RJBri. Advances in the applications of polyhydroxyalkanoate nanoparticles for novel drug delivery system. 2013;2013.
5. Tharanathan RJTifs, technology. Biodegradable films and composite coatings: past, present and future. 2003;14(3):71-8.
6. Sabir MI, Xu X, Li LJJoms. A review on biodegradable polymeric materials for bone tissue engineering applications. 2009;44(21):5713-24.
7. Chen G-Q, Wu QJB. The application of polyhydroxyalkanoates as tissue engineering materials. 2005;26(33):6565-78.
8. Lizarraga-Valderrama L, Panchal B, Thomas C, Boccaccini A, Roy IJBFNfAD, Therapies. Biomedical applications of polyhydroxyalkanoates. 2016:339-83.
9. Koller MJM. Biodegradable and biocompatible polyhydroxy-alkanoates (PHA): Auspicious microbial macromolecules for pharmaceutical and therapeutic applications. 2018;23(2):362.
10. Shi J, Votruba AR, Farokhzad OC, Langer RJNl. Nanotechnology in drug delivery and tissue engineering: from discovery to applications. 2010;10(9):3223-30.
11. Liu L, Liu J, Wang Y, Yan X, Sun DDJNJoC. Facile synthesis of monodispersed silver nanoparticles on graphene oxide sheets with enhanced antibacterial activity. 2011;35(7):1418-23.
12. Castro-Mayorga JL, Freitas F, Reis M, Prieto MA, Lagaron JJIjobm. Biosynthesis of silver nanoparticles and polyhydroxybutyrate nanocomposites of interest in antimicrobial applications. 2018;108:426-35.

13. Hackenberg S, Scherzed A, Kessler M, Hummel S, Technau A, Froelich K, et al. Silver nanoparticles: evaluation of DNA damage, toxicity and functional impairment in human mesenchymal stem cells. 2011;201(1):27-33.

14. Suresh AK, Pelletier DA, Wang W, Morrell-Falvey JL, Gu B, Doktycz MJJL. Cytotoxicity induced by engineered silver nanocrystallites is dependent on surface coatings and cell types. 2012;28(5):2727-35.

15. Wuithschick M, Paul B, Bienert R, Sarfraz A, Vainio U, Sztucki M, et al. Size-controlled synthesis of colloidal silver nanoparticles based on mechanistic understanding. 2013;25(23):4679-89.

16. Levard C, Hotze EM, Lowry GV, Brown Jr GEJEs, technology. Environmental transformations of silver nanoparticles: impact on stability and toxicity. 2012;46(13):6900-14.

17. Riehemann K, Schneider SW, Luger TA, Godin B, Ferrari M, Fuchs HJACIE. Nanomedicine—challenge and perspectives. 2009;48(5):872-97.

18. Saji VS, Choe HC, Yeung KWJIJoN, Biomaterials. Nanotechnology in biomedical applications: a review. 2010;3(2):119-39.

19. Bhatia S. Nanoparticles types, classification, characterization, fabrication methods and drug delivery applications. Natural polymer drug delivery systems: Springer; 2016. p. 33-93.

20. Xiao K, Li Y, Luo J, Lee JS, Xiao W, Gonik AM, et al. The effect of surface charge on in vivo biodistribution of PEG-oligocholic acid based micellar nanoparticles. 2011;32(13):3435-46.

21. Wang L, Wang L, Luo J, Fan Q, Suzuki M, Suzuki IS, et al. Monodispersed core− shell Fe_3O_4@ Au nanoparticles. 2005;109(46):21593-601.

22. Bhatia S. Natural polymer drug delivery systems: Springer; 2016.

23. Fadeel B, Garcia-Bennett AEJAddr. Better safe than sorry: understanding the toxicological properties of inorganic nanoparticles manufactured for biomedical applications. 2010;62(3):362-74.

24. Raj S, Jose S, Sumod U, Sabitha MJJop, sciences b. Nanotechnology in cosmetics: Opportunities and challenges. 2012;4(3):186.

25. Chen W, Zhang JZ, Joly AGJJon, nanotechnology. Optical properties and potential applications of doped semiconductor nanoparticles. 2004;4(8):919-47.

26. Marslin G, Selvakesavan RK, Franklin G, Sarmento B, Dias ACJIjon. Antimicrobial activity of cream incorporated with silver nanoparticles biosynthesized from Withania somnifera. 2015;10:5955.

27. De Jong WH, Borm PJJIjon. Drug delivery and nanoparticles: applications and hazards. 2008;3(2):133.

28. Bumbudsanpharoke N, Choi J, Ko SJJon, nanotechnology. Applications of nanomaterials in food packaging. 2015;15(9):6357-72.

29. Lu H, Wang J, Stoller M, Wang T, Bao Y, Hao HJAiMS, et al. An overview of nanomaterials for water and wastewater treatment. 2016;2016.

30. Araújo R, Castro ACM, Fiúza AJMTP. The use of nanoparticles in soil and water remediation processes. 2015;2(1):315-20.

31. Ochiai T, Fujishima AJJoP, reviews pCP. Photoelectrochemical properties of TiO2 photocatalyst and its applications for environmental purification. 2012;13(4):247-62.

32. Song D, Li M, Wang T, Fu P, Li Y, Jiang B, et al. Dye-sensitized solar cells using nanomaterial/PEDOT–PSS composite counter electrodes: effect of the electronic and structural properties of nanomaterials. 2014;293:26-31.

33. Ilium L, Davis S, Wilson C, Thomas N, Frier M, Hardy JJIjop. Blood clearance and organ deposition of intravenously administered colloidal particles. The effects of particle size, nature and shape. 1982;12(2-3):135-46.

34. Olson EJJoGC. Particle shape factors and their use in image analysis part 1: theory. 2011;15(3):85.

35. Guisbiers G, Mejía-Rosales S, Leonard Deepak FJJoN. Nanomaterial properties: size and shape dependencies. 2012;2012.

36. Kumbhakar P, Ray SS, Stepanov ALJJoN. Optical properties of nanoparticles and nanocomposites. 2014;2014.

37. Haider M, Mehdi MJIJoS, Research E. Study of morphology and Zeta potential analyzer for silver nanoparticles. 2014;5(7):381-5.

38. Srikar SK, Giri DD, Pal DB, Mishra PK, Upadhyay SNJG, Chemistry S. Green synthesis of silver nanoparticles: a review. 2016;6(01):34.

39. Iravani S, Korbekandi H, Mirmohammadi SV, Zolfaghari BJRips. Synthesis of silver nanoparticles: chemical, physical and biological methods. 2014;9(6):385.

40. Iqtedar M, Aslam M, Akhyar M, Shehzaad A, Abdullah R, Kaleem AJPB, et al. Extracellular biosynthesis, characterization, optimization of silver nanoparticles

(AgNPs) using Bacillus mojavensis BTCB15 and its antimicrobial activity against multidrug resistant pathogens. 2019;49(2):136-42.

41. Schneidewind H, Schüler T, Strelau KK, Weber K, Cialla D, Diegel M, et al. The morphology of Ag NPs prepared by enzyme-reduction. 2012;3(1):404-14.

42. Kagithoju S, Godishala V, Nanna RSJB. Eco-friendly and green synthesis of silver nanoparticles using leaf extract of Strychnos potatorum Linn. F. and their bactericidal activities. 2015;5(5):709-14.

43. Perala SRK, Kumar SJL. On the mechanism of metal nanoparticle synthesis in the Brust–Schiffrin method. 2013;29(31):9863-73.

44. Labouta HI, Schneider MJNN, Biology, Medicine. Interaction of inorganic NPs with the skin barrier: current status and critical review. 2013;9(1):39-54.

45. Zhou W, Ma Y, Yang H, Ding Y, Luo XJIjon. A label-free biosensor based on silver nanoparticles array for clinical detection of serum p53 in head and neck squamous cell carcinoma. 2011;6:381.

46. He Y, Du Z, Ma S, Liu Y, Li D, Huang H, et al. Effects of green-synthesized silver nanoparticles on lung cancer cells in vitro and grown as xenograft tumors in vivo. 2016;11:1879.

47. Sarkar K, Banerjee SL, Kundu PP, Madras G, Chatterjee KJJoMCB. Biofunctionalized surface-modified silver nanoparticles for gene delivery. 2015;3(26):5266-76.

48. Panáček A, Smékalová M, Kilianová M, Prucek R, Bogdanová K, Večeřová R, et al. Strong and nonspecific synergistic antibacterial efficiency of antibiotics combined with silver nanoparticles at very low concentrations showing no cytotoxic effect. 2016;21(1):26.

49. Dakal TC, Kumar A, Majumdar RS, Yadav VJFim. Mechanistic basis of antimicrobial actions of silver nanoparticles. 2016;7:1831.

50. Archer NK, Mazaitis MJ, Costerton JW, Leid JG, Powers ME, Shirtliff MEJV. S aureus biofilms: properties, regulation, & roles in human disease. 2011;2(5):445-59.

51. Rasamiravaka T, Labtani Q, Duez P, El Jaziri MJBri. The formation of biofilms by Pseudomonas aeruginosa: a review of the natural and synthetic compounds interfering with control mechanisms. 2015;2015.

52. Vandeputte C, Guizon I, Genestie-Denis I, Vannier B, Lorenzon GJCb, toxicology. A microtiter plate assay for total glutathione and glutathione disulfide

contents in cultured/isolated cells: performance study of a new miniaturized protocol. 1994;10(5-6):415-21.

53. Kalyanaraman B, Darley-Usmar V, Davies KJ, Dennery PA, Forman HJ, Grisham MB, et al. Measuring reactive oxygen and nitrogen species with fluorescent probes: challenges and limitations. 2012;52(1):1-6.

54. Faulkner K, Fridovich IJFRB, Medicine. Luminol and lucigenin as detectors for O2ṡ−. 1993;15(4):447-51.

55. Williams SF, Martin DP, Horowitz DM, Peoples OPJIjobm. PHA applications: addressing the price performance issue: I. Tissue engineering. 1999;25(1-3):111-21.

56. Van Viet P, Sang TT, Bich NHN, Thi CMJJoP, Biology PB. An improved green synthesis method and Escherichia coli antibacterial activity of silver nanoparticles. 2018;182:108-14.

57. Yalcin S, Khodadust R, Unsoy G, Ceren Garip I, Didem Mumcuoglu Z, Gunduz UJS, et al. Synthesis and characterization of polyhydroxybutyrate coated magnetic nanoparticles: Toxicity analyses on different cell lines. 2015;45(5):700-8.

58. Yadav R, Balasubramanian K, Wang XJRa. Encapsulation of gold nanoparticles with PHB based on coffee ring effect. 2015;5(24):18501-5.

59. Sasikumar P, Ayyasamy PJIJCMAS. Design and characterization of poly-hydroxy butyric acid (PHB) based polymeric nanoparticles for controlled release of doxorubicin for cancer treatment. 2015;4(12):311-7.

60. Mostafa MJJoR, Chemistry N. Synthesis of nanosilver by the hydrothermal method and its application for radioiodine sorption from alkaline solution. 2015;304(3):1153-62.

61. Yang J, Pan JJAM. Hydrothermal synthesis of silver nanoparticles by sodium alginate and their applications in surface-enhanced Raman scattering and catalysis. 2012;60(12):4753-8.

62. Sato-Berrú R, Redón R, Vázquez-Olmos A, Saniger JMJJoRSAIJfOWiaAoRS, Including Higher Order Processes,, Brillouin a, Scattering R. Silver nanoparticles synthesized by direct photoreduction of metal salts. Application in surface-enhanced Raman spectroscopy. 2009;40(4):376-80.

63. Pandian SRK, Deepak V, Kalishwaralal K, Muniyandi J, Rameshkumar N, Gurunathan SJC, et al. Synthesis of PHB nanoparticles from optimized medium

utilizing dairy industrial waste using Brevibacterium casei SRKP2: a green chemistry approach. 2009;74(1):266-73.

64. Courrol LC, de Oliveira Silva FR, Gomes LJC, Physicochemical SA, Aspects E. A simple method to synthesize silver nanoparticles by photo-reduction. 2007;305(1-3):54-7.

65. Eustis S, Krylova G, Eremenko A, Smirnova N, Schill AW, El-Sayed MJP, et al. Growth and fragmentation of silver nanoparticles in their synthesis with a fs laser and CW light by photo-sensitization with benzophenone. 2005;4(1):154-9.

66. Abid J-P, Wark A, Brevet P-F, Girault HJCC. Preparation of silver nanoparticles in solution from a silver salt by laser irradiation. 2002(7):792-3.

67. Lu P-J, Fu W-E, Huang S-C, Lin C-Y, Ho M-L, Chen Y-P, et al. Methodology for sample preparation and size measurement of commercial ZnO nanoparticles. 2018;26(2):628-36.

68. Cymes BA, Krekeler MP, Nicholson KN, Grigsby JDJEES. A transmission electron microscopy (TEM) study of silver nanoparticles associated with mine waste from New Caledonian nickel deposits: potential origins of silver toxicity in a World Heritage Site. 2017;76(18):640.

69. Palestrant D, Holzknecht ZE, Collins BH, Parker W, Miller SE, Bollinger RRJUp. Microbial biofilms in the gut: visualization by electron microscopy and by acridine orange staining. 2004;28(1):23-7.

70. Philip DJSAPAM, Spectroscopy B. Honey mediated green synthesis of silver nanoparticles. 2010;75(3):1078-81.